

Scuola di Scienze
Dipartimento di Fisica e Astronomia
Corso di Laurea in Fisica

Analytical and numerical study of polarons through a DFT calculation in rutile TiO₂

Relatore:

Prof. Cesare Franchini

Presentata da:

Nicolò Montalti

Correlatore:

Lorenzo Varrassi

Anno Accademico 2021/2022

Sommario

Lo scopo di questa tesi è di introdurre il concetto di polarone e di presentare un calcolo DFT di uno small polaron nel rutile. Nei primi capitoli si analizzano gli small e large polarons con un approccio analitico, basato sulle Hamiltoniane di Holstein e di Fröhlich. Il formalismo matematico e le basi fisiche necessarie vengono introdotte nel primo capitolo.

Nella seconda parte della tesi, si introduce la Density Functional Theory, una sua correzione (DFT+U) e la sua implementazione in VASP. Il calcolo numerico è poi descritto e discusso a un livello qualitativo. La soluzione polaronica è confrontata con un elettrone delocalizzato nel materiale.

Il calcolo ha evidenziato come il polaron crea un nuovo stato energetico 0.70 eV sotto la banda di conduzione. Il nuovo livello energetico era visibile sia nella struttura a bande, sia nel grafico della densità degli stati. L'elettrone si localizza su un atomo di titanio, distorcendo il reticolo circostante. In particolare, i quattro atomi più vicini al titanio si allontano di 0.085 Å, mentre i due atomi di ossigeno più distanti di 0.023 Å.

I risultati sono qualitativamente compatibili con la letteratura. Futuri sviluppi del lavoro possono cercare di migliorare la precisione del calcolo, proponendo un confronto quantitativo.

Abstract

The aim of this thesis is to introduce the polaron concept and to perform a DFT numerical calculation of a small polaron in rutile TiO_2 . In the first chapters we present an analytical study of small and large polarons, based on the Holstein and Fröhlich Hamiltonians. The necessary mathematical formalism and physics fundamentals are briefly reviewed in the first chapter.

In the second part of the thesis, Density Functional Theory is introduced together with the DFT+U correction and its implementation in VASP. The actual calculation is then described and discussed at qualitative level. The polaronic solution is compared in detail with a delocalized electron.

The calculation showed how the polaron creates a new energy level 0.70 eV under the conduction band. The energy level was visible both in the band structure diagram and in the density of states diagram. The electron localizes on a Ti atom, distorting the surrounding lattice. In particular, the four oxygen atoms closer to the titanium atom are displaced by 0.085 Å outwards, whereas the two further oxygen atoms by 0.023 Å.

The results are compatible, at a qualitative level, with the literature. Further developments of this work may try to improve the precision of the results and compare them with the literature.

ACKNOWLEDGEMENTS

This work would have not been possible without the help and the support of many people, more than this page could contain. Not only the ones that have contributed directly or indirectly to it in the past months, but everyone I met along the path of taking this degree.

First of all, I want to thank my supervisor Prof. Cesare Franchini for giving me the opportunity of working on such an interesting topic. I am grateful for the time he dedicated to me and to this work. I also want to thank Lorenzo Varrassi for the help he gave me understanding DFT and VASP. I would not have been able to conclude this work without his advices. Finally, I am grateful to the Department of Physics of the University of Bologna for letting me use their HPC Cluster for running my calculations.

I want to thank my family, especially my parents and grandparents, for believing in me and encouraging my passion in Physics. This work is dedicated to my mother, who could not fulfill the dream of studying this subject like me. I thank my father for his patience, his support and for feeding my curiosity since I was child. I am grateful to my sisters, for bearing me talking about my work, and to my grandparents, for their support and interest in my studies.

Between my friends, a special thanks goes to Mattia, Adriano, Alessandro and Pietro, for making me feel home in a city it has never been really mine. I will never be able to repay them for their heartwarming hospitality. I have to thank Alessandro in particular for all the time he dedicated to listening to me, and Claudia and Lorenzo for their friendship and the time we spent together.

I also want to thank Lorenzo and Alice, who have been two invaluable peers in the path to obtaining this degree. They have had a major role in keeping my curiosity and my enthusiasm always high in the past years. They have been among the few people I could actually discuss my work with, and help me when I needed it.

A final, heartfelt thanks goes to Edoardo, Thomas, Jakob F., Jakob S., Samira, Riley, and all the other wonderful people I met in Groningen. With them, I spent the best months of my studies. Each of them changed me in their own way, making me discover a whole new me I could have not found otherwise. I am sure we will meet again many times all over Europe.

I hope that all these people will be as proud of this work as I am, even the ones who might not understand it.

CONTENTS

Introduction	viii
1 Review of fundamentals	1
1.1 Second quantization	1
1.1.1 Occupation number representation	1
1.1.2 Creation and annihilation operators	3
1.1.3 Commutation relations	5
1.1.4 Dynamical variables	6
1.2 Electrons and phonons in crystals	7
1.2.1 Crystal lattice	7
1.2.2 Electrons in crystals	8
1.2.3 Tight binding model	10
1.2.4 Phonons	12
1.2.5 Electron-phonon interaction	14
2 The polaron problem	18
2.1 Landau-Pekar model	18
2.2 Fröhlich polarons	20
2.2.1 Derivation of the Fröhlich Hamiltonian	20
2.2.2 Weak coupling limit	24
2.2.3 Strong coupling limit	27
2.3 Holstein polarons	28
2.3.1 Derivation of the Holstein Hamiltonian	29
2.3.2 Weak coupling limit	31
2.4 Small and large polarons	32
3 Density Functional Theory	35
3.1 Introduction to DFT	35
3.1.1 Ground state and density functional formalism	35
3.1.2 The Kohn-Sham Equations	37
3.1.3 DFT corrections: DFT+U	40
3.2 Implementation	41
3.3 Vienna Ab-initio Simulation Package	43
4 Simulation of a small polaron in rutile	46
4.1 Procedure	46
4.1.1 DFT and DFT+U calculation on rutile	46
4.1.2 Electron localization	48
4.1.3 Polaron	50
4.2 Results	50
4.2.1 DFT and DFT+U calculation on rutile	50

4.2.2	Electron localization	52
4.2.3	Polaron	53
5	Conclusions	56

LIST OF FIGURES

Figure 1	Charge isosurfaces of a small and a large polaron	34
Figure 2	Pseudopotentials	43
Figure 3	Rutile unit cell and supercell	47
Figure 4	Brillouin zone of a tetragonal system	48
Figure 5	Band structure and DOS of the TiO ₂ rutile unit cell	51
Figure 6	Band structure and DOS of the TiO ₂ rutile supercell	52
Figure 7	Band structure and DOS of the TiO ₂ rutile supercell with an extra electron	54
Figure 8	Supercell with the isosurface of the charge density projected on the extra-electron band	55
Figure 9	Central atom with the isosurface of the charge density projected on the extra-electron band	55

INTRODUCTION

Lev Landau was the first to propose the concept of an auto-localized electron in a crystal in a 1933 paper [1]. The idea was then developed by Pekar, who considered a single electron interacting with a dielectric continuum medium [2, 3]. He was the first to use the term *polaron* to define an electron that localizes itself in a potential well, self-generated by the polarization of the material. This interaction was shown to cause an enhancement of the effective mass and a localization of the wavefunction [4]. In their work, Landau and Pekar used a quantum mechanical description of the electron and a classical description of the medium. A full quantum mechanical description was then developed by Fröhlich [5] and Holstein [6], who formalized the distinction between large and small polarons.

Fröhlich considered an electron in a continuum, polarizable medium. The electron is assumed to interact only with longitudinal optical phonons. The interaction gives rise to the polarization of the material, which generates a potential well in which the electron localizes. Since the medium is treated as a continuum, the result is valid only for large polarons, that are polarons with an effective radius larger than the lattice constant. On the other hand, Holstein considered short-range electron-phonon interactions, resulting from the coupling between a carrier and the strain where it resides. Holstein theory takes into account the discreteness of the lattice, and it is used to describe small polarons, that are polarons with an effective radius smaller than the lattice constant.

All the attempts find analytical solutions to Fröhlich Hamiltonian have been fruitless, and Holstein Hamiltonian is exactly solvable only in the two-site case [7]. Approximation techniques and numerical simulations are unavoidable. Good results have been achieved with the Diagrammatic Quantum Monte Carlo method to solve both the Fröhlich and Holstein Hamiltonians [8, 9]. For small polarons, DFT+U methods have also proven to be applicable [10]. A rigorous, ab initio computational theory of polarons was recently developed by Feliciano Giustino and colleagues combining the Landau–Pekar model with DFT [11].

OUTLINE

The aim of this thesis is to give an introductory analytical description of polarons and to perform a numerical simulation of a small polaron in rutile. The focus of the analytical discussion is to derive Holstein and Fröhlich Hamiltonians. The numerical calculation aims to simulate a small polaron in rutile TiO_2 . The results are discussed at a qualitative level.

In Chapter 1, we will introduce the mathematical formalism and physical laws necessary for the study of polarons. We will start by reviewing the second quantization formalism, and we will use it to describe electrons and phonons in crystals. Electrons and phonons are firstly studied as non-interacting systems. Then, their interaction, essential for the description of polarons, is investigated as well.

In Chapter 2 the theory of polarons is explained starting from the original Landau-Pekar model. Then, Fröhlich and Holstein Hamiltonians are derived and solved in the small and large coupling regimes using perturbation theory and variational principles. Lastly, small and large polarons properties are discussed and compared.

In Chapter 3 Density Functional Theory (DFT) is presented. The theory behind it is explained together with some of its problems. An extension of it, DFT+U, is also introduced to solve some inaccuracies. Lastly, its implementation is discussed, focusing on VASP, the Vienna Ab-initio Simulation Package.

In Chapter 4 the simulation of a small polaron in TiO_2 is presented. The whole simulation process is described, and the results are discussed. The polaronic solution is compared to a delocalized one, with particular emphasis on the density of states, band structure and charge isosurfaces.

REVIEW OF CONDENSED MATTER PHYSICS FUNDAMENTALS

Before discussing polarons and their properties, we offer a brief review of some fundamentals of condensed matter physics. We start by discussing the second quantization formalism, which will be used extensively in the rest of the thesis. Then, we will briefly describe the behaviour of electrons and phonons in materials, included their interaction, which serves as a basis for the description of polarons.

1.1 SECOND QUANTIZATION

Second quantization, also referred to as occupation number representation, is a formalism used to describe and analyse quantum many-body systems. The key ideas of this method were introduced in 1927 by Paul Dirac [12], and were later developed by Vladimir Fock and Pascual Jordan [13]. The key idea of second quantization is to represent states of a many-body system as elements of a Fock space. The elements of a Fock space are labelled only by the number of particles in the different single-particle states. This approach is particularly useful because it allows us to neglect the individual single-particle states, and focus only on the whole system.

1.1.1 Occupation number representation

In condensed matter physics we often have to deal with systems of many particles. We can describe such a system starting from the wavefunctions of the single particles $|k\rangle$, where the particle is in the eigenstate of eigenvalue k of an operator \hat{K} . We suppose this set of vectors to be orthonormal. We could initially write the total state vector as the product of the single ones.

$$|\Psi\rangle = |k_1\rangle |k_2\rangle \dots |k_N\rangle \quad (1.1)$$

However, the former expression does not take into account the indistinguishability of quantum particles. In fact, the physics of the system must be invariant under the exchange of two particles. This is possible only if $|\Psi\rangle$ is symmetric or antisymmetric for the exchange of two particles. The former case is true for bosons, the latter for fermions.

In order to satisfy this condition, we have to modify Eq. (1.1). An appropriate linear combination of the products of the single kets, compatible with the symmetry constraints required by Bose and Fermi statistics is given by

$$|\Psi\rangle = |k_1, k_2, \dots, k_N\rangle = \sqrt{\frac{1}{N!}} \sum_P \xi^P |P[k_1]\rangle |P[k_2]\rangle \dots |P[k_N]\rangle \quad (1.2)$$

where the sum is taken over the $N!$ permutations P of k_1, k_2, \dots, k_N . The constant ξ is equal to 1 for bosons and -1 for fermions. For fermions, $\xi^P = 1$ for even permutations and $\xi^P = -1$ for odd permutations. This construction assures that the total wavefunction is symmetric for the exchange of two bosons and antisymmetric for the exchange of two fermions. It is important to notice that Eq. (1.2) has an ambiguity in the phase of the final vector. To remove it, we chose the permutation to be even when $k_1 < k_2 < \dots < k_N$.

It is useful to compute the product of a basis bra and a basis ket of two total state vectors.

$$\begin{aligned} \langle m_1, \dots, m_N | k_1, \dots, k_N \rangle &= \frac{1}{N!} \\ &= \sum_P \sum_{P'} \xi^{P+P'} \langle P[m_1] | \langle P[m_2] | \dots \langle P[m_N] | \times |P'[k_1]\rangle |P'[k_2]\rangle \dots |P'[k_N]\rangle \\ &= \sum_{P''} \xi^{P''} \langle m_1 | P''[k_1]\rangle \dots \langle m_N | P''[k_N]\rangle \\ &= \left| \begin{array}{cccc} \langle m_1 | k_1 \rangle & \langle m_1 | k_2 \rangle & \dots & \langle m_1 | k_N \rangle \\ \langle m_2 | k_2 \rangle & \langle m_2 | k_2 \rangle & \dots & \langle m_2 | k_N \rangle \\ \dots & \dots & \dots & \dots \\ \langle m_N | k_1 \rangle & \langle m_N | k_2 \rangle & \dots & \langle m_N | k_N \rangle \end{array} \right|_\xi \quad (1.3) \end{aligned}$$

where $|\cdot|_{\xi=-1}$ represents a determinant and $|\cdot|_{\xi=1}$ a permanent (a determinant with all positive signs). Given the orthonormality of the single state kets, the only terms of the sum that differ from zero are the ones where

$$P''\{k_1, \dots, k_N\} = \{m_1, \dots, m_N\} \quad (1.4)$$

If a state is composed of n_j bosons in the state k_j , the norm squared of the state vector will be equal to the total number of identical permutations

$$\langle k_1, \dots, k_N | k_1, \dots, k_N \rangle = n_1! n_2! \dots n_N! \quad (1.5)$$

Thus, the normalized state vector is

$$|k_1, \dots, k_N\rangle_n = \frac{1}{\sqrt{n_1! n_2! \dots n_N!}} |k_1, \dots, k_N\rangle \quad (1.6)$$

The case of fermions is easier. Since n_j can only be either 1 or 0, there is only one identical permutation and the state is already normalized.

Given the indistinguishability of the particles, a simpler way to describe this state vector is using only the number n_j of particles that are in the state k_j .

$$|n_1, n_2, \dots, n_i, \dots\rangle = |k_1, \dots, k_N\rangle_n \quad (1.7)$$

where k_j is repeated n_j times. This eliminates the inconvenience of having multiple kets describing the same state as we had before. This representation is called occupation number representation, and the kets are said to be elements of the Fock space.

Two special cases of states in the Fock space are the following. The vacuum state

$$|0, 0, \dots, 0\rangle = |0\rangle \quad (1.8)$$

is a state with no particles in any single-particle states, and

$$|0, 0, \dots, n_i = 1, \dots\rangle = |k_i\rangle \quad (1.9)$$

is a state with exactly one particle in the k_i state.

1.1.2 Creation and annihilation operators

Now that we have defined the basis kets, we can introduce two operators that are used to transform the states. We define the *creation operator* as

$$\hat{a}_i^\dagger |k_1, k_2, \dots\rangle = |k_i, k_1, k_2, \dots\rangle \quad (1.10)$$

Below we show several properties that derive from this definition, but its essential role can be understood applying it to the vacuum state.

$$\hat{a}_i^\dagger |0\rangle = |k_i\rangle \quad (1.11)$$

Its effect is to add a particle in k_i state to the system. It is easy to interpret its adjoint as an *annihilation operator*, in fact

$$1 = \langle k_i | k_i \rangle = \langle 0 | \hat{a}_i \hat{a}_i^\dagger | 0 \rangle = \langle 0 | \hat{a}_i | k_i \rangle \quad (1.12)$$

which implies that

$$\hat{a}_i |k_i\rangle = |0\rangle \quad (1.13)$$

We now try to prove these properties on a general basis ket. We consider the transition matrix element

$$\begin{aligned} \mathcal{A} &= \langle m_1, \dots, m_{N-1} | \hat{a}_i | k_1, \dots, k_N \rangle = \\ &= \langle k_1, \dots, k_N | \hat{a}_i^\dagger | m_1, \dots, m_{N-1} \rangle^* = \langle k_1, \dots, k_N | k_i, m_1, \dots, m_{N-1} \rangle^* \end{aligned} \quad (1.14)$$

Using Eq. (1.3) we write it as the determinant

$$\mathcal{A} = \begin{vmatrix} \langle k_1 | k_i \rangle & \langle k_1 | m_1 \rangle & \dots & \langle k_1 | m_{N-1} \rangle \\ \langle k_2 | k_i \rangle & \langle k_2 | m_1 \rangle & \dots & \langle k_2 | m_{N-1} \rangle \\ \dots & \dots & \dots & \dots \\ \langle k_N | k_i \rangle & \langle k_N | m_1 \rangle & \dots & \langle k_N | m_{N-1} \rangle \end{vmatrix}_{\xi}^* \quad (1.15)$$

and developing it along the first column

$$\begin{aligned} \mathcal{A} &= \left(\sum_{j=1}^N \xi^{j+1} \langle k_j | k_i \rangle \begin{vmatrix} \langle k_1 | m_1 \rangle & \dots & \langle k_1 | m_{N-1} \rangle \\ \langle k_2 | m_1 \rangle & \dots & \langle k_2 | m_{N-1} \rangle \\ \dots & (no \ k_j) & \dots \\ \langle k_N | m_1 \rangle & \dots & \langle k_N | m_{N-1} \rangle \end{vmatrix}_{\xi} \right)^* \\ &= \sum_{j=1}^N \xi^{j+1} \langle k_i | k_j \rangle \langle k_1, \dots, (no \ k_j), k_N | m_1, \dots, m_{N-1} \rangle^* \\ &= \sum_{j=1}^N \xi^{j+1} \delta_{k_i k_j} \langle m_1, \dots, m_{N-1} | k_1, \dots, (no \ k_j), k_N \rangle \quad (1.16) \end{aligned}$$

Confronting Eq. (1.16) with Eq. (1.14) we conclude

$$\begin{aligned} \hat{a}_i |k_1, \dots, k_N\rangle &= \sum_{j=1}^N \xi^{j+1} \langle k_i | k_j \rangle |k_1, \dots, (no \ k_j), k_N\rangle \\ &= \sum_{j=1}^N \xi^{j+1} \delta_{k_i k_j} |k_1, \dots, (no \ k_j), k_N\rangle \quad (1.17) \end{aligned}$$

If k_i is not present in $|k_1, \dots, k_N\rangle$, $\delta_{k_i k_j} = 0$ and overall $\hat{a}_i |k_1, \dots, k_N\rangle = 0$. On the other hand, if k_i is included in the ket n_i times, there will be n_i non-null terms in the sum. Thus, in the case of bosons,

$$\hat{a}_i |k_1, \dots, k_N\rangle = n_i |k_1, \dots, (one \ less \ k_i), k_N\rangle \quad (1.18)$$

We can use Eq. (1.7) to express the last relation in the occupation number representation.

$$\begin{aligned} \hat{a}_i |n_1, n_2, \dots, n_i, \dots\rangle &= \hat{a}_i |k_1, \dots, k_N\rangle_n \\ &= \hat{a}_i \left(\prod_{j=1}^N \sqrt{n_j!} \right)^{-1} |k_1, \dots, k_N\rangle = n_i \left(\prod_{j=1}^N \sqrt{n_j!} \right)^{-1} |k_1, \dots, (one \ less \ k_i), k_N\rangle \\ &= \sqrt{n_i} |k_1, \dots, (one \ less \ k_i), k_N\rangle_n = \sqrt{n_i} |n_1, n_2, \dots, n_i - 1, \dots\rangle \quad (1.19) \end{aligned}$$

The same argument, developed for the creation operator \hat{a}_i^\dagger , leads to

$$\hat{a}_i^\dagger |n_1, n_2, \dots, n_i, \dots\rangle = \sqrt{n_i + 1} |n_1, n_2, \dots, n_i + 1, \dots\rangle \quad (1.20)$$

For fermions, the occupation numbers can either be 1 or 0. The creation operator \hat{a}_i^\dagger returns zero if $n_i = 1$ and a phase factor of ± 1 if $n_i = 0$. The annihilation operator \hat{a}_i does the opposite.

We can define another useful operator, the number operator $\hat{N}_i = \hat{a}_i^\dagger \hat{a}_i$. If we apply it to a basis ket of a system of bosons

$$\begin{aligned}\hat{N}_i |n_1, n_2, \dots, n_i, \dots\rangle &= \hat{a}_i^\dagger \hat{a}_i |n_1, n_2, \dots, n_i, \dots\rangle \\ &= \hat{a}_i^\dagger \sqrt{n_i} |n_1, n_2, \dots, n_i - 1, \dots\rangle = n_i |n_1, n_2, \dots, n_i, \dots\rangle\end{aligned}\quad (1.21)$$

The number operator \hat{N}_i , as the name suggests, returns the number of bosons in the state k_i in the system

1.1.3 Commutation relations

All the properties of the creation and annihilation operators can be deduced from their (anti)commutation relations, which will be derived in this section. Applying $\hat{a}_{k'}^\dagger \hat{a}_k^\dagger$ on a basis ket, using Eq. (1.10)

$$\begin{aligned}\hat{a}_{k'}^\dagger \hat{a}_k^\dagger |k_1, k_2, \dots\rangle &= |k', k, k_1, k_2, \dots\rangle \\ &= \xi |k, k', k_1, k_2, \dots\rangle = \xi \hat{a}_k^\dagger \hat{a}_{k'}^\dagger |k_1, k_2, \dots\rangle\end{aligned}\quad (1.22)$$

which implies the (anti)commutation relation

$$\hat{a}_k^\dagger \hat{a}_{k'}^\dagger - \xi \hat{a}_{k'}^\dagger \hat{a}_k^\dagger = [\hat{a}_k^\dagger, \hat{a}_{k'}^\dagger]_\xi = 0 \quad (1.23)$$

where $[A, B]_{-1} = \{A, B\} = AB + BA$ and $[A, B]_1 = AB - BA$. We see that for bosons the creation operators always commute, while for fermions they anti-commute.

Let's now investigate the commutator of a creation and an annihilation operator. Using Eq. (1.10) and Eq. (1.17)

$$\begin{aligned}\hat{a}_{k'} \hat{a}_k^\dagger |k_1, k_2, \dots\rangle &= \hat{a}_{k'} |k, k_1, k_2, \dots\rangle \\ &= \langle k' | k \rangle |k_1, k_2, \dots\rangle + \sum_j \xi^j \langle k' | k_j \rangle |k, k_1, k_2, (\text{no } k_j) \dots\rangle\end{aligned}\quad (1.24)$$

$$\begin{aligned}\hat{a}_k^\dagger \hat{a}_{k'} |k_1, k_2, \dots\rangle &= \hat{a}_k^\dagger \sum_j \xi^{j+1} \langle k' | k_j \rangle |k_1, k_2, (\text{no } k_j) \dots\rangle \\ &= \sum_j \xi^{j+1} \langle k' | k_j \rangle |k, k_1, k_2, (\text{no } k_j) \dots\rangle\end{aligned}\quad (1.25)$$

thus

$$(\hat{a}_{k'} \hat{a}_k^\dagger - \xi \hat{a}_k^\dagger \hat{a}_{k'}) = \langle k' | k \rangle |k_1, k_2, \dots\rangle \quad (1.26)$$

and

$$[\hat{a}_{k'}, \hat{a}_k^\dagger]_\xi = \langle k' | k \rangle = \delta_{kk'} \quad (1.27)$$

The previous equation is of fundamental importance in second quantization formalism. If we have a set of single-state basis kets $|k\rangle$ and we define a creation and annihilation operator that satisfy Eq. (1.27), we obtain multi-particle basis kets $|k_1, k_2, \dots\rangle$ that automatically satisfy the symmetry condition of Fermi and Bose statistics. The kets can then be expressed in the more compact occupation number representation $|n_1, n_2, \dots\rangle$.

1.1.4 Dynamical variables

The final aim of second-quantization is to express every operator in terms of the creation and annihilation operators. The action of every operator can be interpreted as a combination of the creation (\hat{a}^\dagger), annihilation (\hat{a}) and counting (\hat{N}) of the particles in the system. This allows us to use Fock states as kets and to simplify our equations. We focus our discussion on additive single-particle operator [14]. Examples are momentum, kinetic energy and single body potentials. In these cases, the total expectation value of the operator is simply given by the sum of the expectation values of the operator applied to the single particles.

Given an operator \hat{K} of eigenkets $|k_i\rangle$, with $\hat{K}|k_i\rangle = k_i|k_i\rangle$, and a state vector

$$|\Psi\rangle = |n_1, n_2, \dots\rangle \quad (1.28)$$

the result of applying \hat{K} to $|\Psi\rangle$ is simply

$$\hat{K}|\Psi\rangle = \left(\sum_i n_i k_i \right) |\Psi\rangle \quad (1.29)$$

Confronting this expression with the definition of the number operator expressed in Eq. (1.21) we can write \hat{K} as

$$\hat{K} = \sum_i k_i \hat{N}_i = \sum_i k_i \hat{a}_i^\dagger \hat{a}_i \quad (1.30)$$

It could happen to have a state ket expressed in a base different from the eigenkets of our operator of interest. If we suppose this base to be formed by $|l_j\rangle$, using the relation of completeness,

$$|k_i\rangle = \sum_j |l_j\rangle \langle l_j | k_i \rangle \quad (1.31)$$

It makes then sense to write

$$\hat{a}_i^\dagger = \sum_j \hat{b}_j^\dagger \langle l_j | k_i \rangle \quad (1.32)$$

which implies

$$\hat{a}_i = \sum_j \hat{b}_j \langle k_i | l_j \rangle \quad (1.33)$$

where operators \hat{b}_j^\dagger and \hat{b}_j create and annihilate the single-particle states $|l_j\rangle$. The result of applying Eq. (1.32) on the vacuum state is then

$$\hat{a}_i^\dagger |0\rangle = \sum_j \hat{b}_j^\dagger \langle l_j | k_i \rangle |0\rangle = \sum_j |l_j\rangle \langle l_j | k_i \rangle = |k_i\rangle \quad (1.34)$$

in agreement with Eq. (1.31).

We are now ready to express the operator \hat{K} in the basis $|l_j\rangle$.

$$\begin{aligned} \hat{K} &= \sum_i k_i \hat{a}_i^\dagger \hat{a}_i = \sum_i k_i \sum_{mn} \hat{b}_m^\dagger \hat{b}_n \langle l_m | k_i \rangle \langle k_i | l_n \rangle \\ &= \sum_{mn} \hat{b}_m^\dagger \hat{b}_n \sum_i \langle l_m | k_i \rangle k_i \langle k_i | l_n \rangle = \sum_{mn} \hat{b}_m^\dagger \hat{b}_n \langle l_m | \left[\hat{K} \sum_i |k_i\rangle \langle k_i| \right] |l_n\rangle \\ &= \sum_{mn} \langle l_m | \hat{K} | l_n \rangle \hat{b}_m^\dagger \hat{b}_n \quad (1.35) \end{aligned}$$

This allows us to write every additive operator in terms of the creation and annihilation operators. For example, it is possible to write the Hamiltonian for a non-interacting system of particles, where the potential and the kinetic energy satisfy the additivity requirement, as

$$\hat{H} = \sum_{mn} \langle l_m | \hat{T} + V_1 | l_n \rangle \hat{b}_m^\dagger \hat{b}_n \quad (1.36)$$

where V_1 is the non-interacting (single particle) potential and \hat{T} the kinetic energy.

1.2 ELECTRONS AND PHONONS IN CRYSTALS

In this section we will briefly describe how free electrons and phonons behave in crystals, starting with a description of the crystal lattice. Initially, the interaction between two electrons and two phonons will not be considered. Eventually, the electron-phonon interaction will be discussed, as this represent the key interaction of the polaron quasiparticle.

1.2.1 Crystal lattice

Solid state physics deals with materials made of huge numbers of atoms, of the order of the Avogadro number. We have just developed a mathematical formalism (second quantization) with which it is possible to treat such systems. However, it is clearly impossible to solve the equations for a general N-body system. Luckily, X-ray diffraction

experiments showed that many solids exhibit particular symmetry properties, useful to simplify the problem.

Many solids, called crystals, are composed by the repetition in space of an identical unit cell. The unit cell is defined as the smallest repeating unit having the full symmetry of the crystal structure. Each unit cell is placed on a point of a Bravais lattice. The Bravais lattice, also referred to as space lattice, describes the geometric arrangement of the lattice points. Given any two points of the lattice, described by the vectors \mathbf{R}_1 and \mathbf{R}_2 , the difference between them is always

$$\mathbf{R}_1 - \mathbf{R}_2 = \mathbf{R}_n \quad (1.37)$$

with $\mathbf{R}_n = n_1 \mathbf{a}_1 + n_2 \mathbf{a}_2 + n_3 \mathbf{a}_3$. The three vectors $\mathbf{a}_1, \mathbf{a}_2, \mathbf{a}_3$ are called basis vectors and n_1, n_2, n_3 are integers. The position of a single atom in the crystal can then be expressed as the sum of its position in the unit cell τ_a and the position of the lattice point \mathbf{R}_n in the crystal

$$\mathbf{R}_n^a = \mathbf{R}_n + \tau_a \quad (1.38)$$

Given the symmetry of the system, every property $f(\mathbf{r})$ of the lattice is invariant under a translation of a lattice vector \mathbf{R}_n

$$f(\mathbf{r} + \mathbf{R}_n) = f(\mathbf{r}) \quad (1.39)$$

We will see that applying this simple principle to the potential generated by the ions of the crystal will have important implications on the description of electrons.

Associated to the Bravais lattice, there is a second lattice called reciprocal lattice. It is defined by three other basis vectors $\mathbf{b}_1, \mathbf{b}_2, \mathbf{b}_3$, with

$$\mathbf{b}_1 = \frac{2\pi}{\Omega} \mathbf{a}_2 \times \mathbf{a}_3 \quad \mathbf{b}_2 = \frac{2\pi}{\Omega} \mathbf{a}_3 \times \mathbf{a}_1 \quad \mathbf{b}_3 = \frac{2\pi}{\Omega} \mathbf{a}_1 \times \mathbf{a}_2 \quad (1.40)$$

where $\Omega = |\mathbf{a}_1 \cdot \mathbf{a}_2 \times \mathbf{a}_3|$ is the volume of the unit cell. A vector in the reciprocal lattice is usually written as $\mathbf{G}_m = m_1 \mathbf{b}_1 + m_2 \mathbf{b}_2 + m_3 \mathbf{b}_3$, where m_1, m_2, m_3 are integers. From Eq. (1.40) it is easy to see that the product of a basis Bravais lattice vector \mathbf{a}_i and a basis reciprocal lattice vector \mathbf{b}_j is

$$\mathbf{a}_i \cdot \mathbf{b}_j = 2\pi \delta_{ij} \quad (1.41)$$

1.2.2 Electrons in crystals

The simplest quantum-mechanical model of electrons in solids is the Sommerfield model. It was developed by Arnold Sommerfeld in 1928 [15], combining the Drude model [16] with Fermi-Dirac statistics. The electrons are treated as quantum non-interacting free particles, which implies that the wavefunctions are plane waves

$$\psi_{\mathbf{k}} = e^{i\mathbf{k} \cdot \mathbf{r}} \quad (1.42)$$

The energy is entirely kinetic, thus the dispersion relation is

$$\epsilon_{\mathbf{k}} = \frac{\hbar k^2}{2m} \quad (1.43)$$

Despite its simplicity, this model is surprisingly good at describing a vast number of physical phenomena. Examples are the Wiedemann–Franz law, electrons heat capacity and electrical conductivity. However, it does not give any explanation for the different properties of conductors, insulators and semiconductors.

To correctly describe the properties of electrons, we have to take into account the potential generated by the ions in the crystal. The interaction is entirely electrical, so the potential is the well known Coulomb potential

$$V_{e-N} = \sum_{i=1}^{N_e} \sum_{j=1}^{N_N} \frac{1}{4\pi\epsilon_0} \frac{-Z_j e^2}{|\mathbf{r}_i - \mathbf{R}_j|} \quad (1.44)$$

where the first sum is extended over all the electrons and the second over the nuclei. It is convenient to divide the electrons in inner core electrons and valence electrons. The formers are tightly bound to the nucleus and occupy closed inner shells. They do not interact with other atoms of the crystal, so the nucleus together with its core electrons can be treated as a positive ion. The valence electrons, belonging to non-closed shells, form chemical bonds with other atoms. Despite this description of electrons being apparently simpler, the potential of interaction between valence electrons and ions cannot be treated as a simple Coulomb potential anymore.

To overcome the complexity of solving a many-body Schrödinger equation with a long range electromagnetic interaction, we leverage the symmetry of the crystal. Recalling our previous discussion, we know that the potential of the ions is translationally invariant:

$$V_{e-I}(\mathbf{r} + \mathbf{R}_n) = V_{e-I}(\mathbf{r}) \quad (1.45)$$

where \mathbf{r} is the position of the electron and \mathbf{R}_n is a Bravais lattice vector. The Schrödinger equation for the periodic potential V_{e-I} is then

$$\hat{H}_{\text{Bloch}} \Psi = \left(-\frac{\hbar^2}{2m} \nabla^2 + V_{e-I} \right) \Psi = \epsilon \Psi \quad (1.46)$$

Block proved in 1929 that the solutions of this problem are the Bloch functions Ψ_{nk} :

$$\hat{H}_{\text{Block}} \Psi_{nk} = \epsilon_n(\mathbf{k}) \Psi_{nk} \rightarrow \Psi_{nk}(\mathbf{r}) = u_{nk}(\mathbf{r}) e^{i\mathbf{k} \cdot \mathbf{r}} \quad (1.47)$$

where u is a function with the same periodicity of V_{e-I} , \mathbf{k} is a wavevector and n is the band index [17]. The plane wave solution showed in Eq. (1.42) is a simple case of Eq. (1.47), where V_{e-I} and u are constant. An important consequence of the Bloch theorem is that the solutions to the Schrödinger equation, even if they are not plane waves, can still be indexed with the quantum number \mathbf{k} , along with the band index n .

Expanding $\epsilon_n(\mathbf{k})$ around $\mathbf{k} = 0$, for an isotropic energy band,

$$\epsilon_n(\mathbf{k}) = \epsilon_n(0) + \frac{\hbar k^2}{2m^*} + \mathcal{O}(k^3) \quad (1.48)$$

where m^* is the effective mass, defined as

$$\frac{1}{m^*} = \frac{1}{\hbar^2} \frac{\partial^2 \epsilon}{\partial k^2} \quad (1.49)$$

Expression (1.48) is formally identical to Eq. (1.43) with m^* in place of m . For small values of k electrons can then be treated as free particles of mass m^* .

We can now define a creation and an annihilation operator $\hat{c}_{n\mathbf{k}}^\dagger, \hat{c}_{n\mathbf{k}}$ as the operators that create and annihilate an electron of quantum numbers (\mathbf{k}, n) . Using Eqs. (1.30) and (1.47), the final non-interacting electron Hamiltonian can be rewritten in second quantization as

$$\hat{H}_{el} = \sum_{n\mathbf{k}} \epsilon_{n\mathbf{k}} \hat{c}_{n\mathbf{k}}^\dagger \hat{c}_{n\mathbf{k}} \quad (1.50)$$

1.2.3 Tight binding model

In solid state physics, the most simple models used to describe electrons are the *nearly-free electrons model* described above and the *tight-binding model*. These two models approach the problem from an almost opposite point of view. If in the *nearly-free electrons model* electrons are treated as free particles, perturbed by the ionic potential, in the *tight-binding model* electrons are treated as tightly bounded to the atoms. We now want to explore the latter, since it is used to describe electrons in the Holstein Hamiltonian.

Since the electrons are tightly bounded to the atoms, we suppose their wavefunction to be a linear combination of the atomic orbitals. The atomic orbitals ϕ_{ta} are functions that satisfy the equation

$$\left(\frac{\mathbf{p}^2}{2m} + V_a(\mathbf{r}) \right) \phi_{ta} = E_{ta} \phi_{ta} \quad (1.51)$$

where V_a is the potential generated by an ion of type a and t is a label for different atomic states. We form a linear combination of atomic orbitals (LCAO) which will be used as a basis to expand the electron wavefunction

$$\phi_k^{ta}(\mathbf{r}) = \frac{1}{\sqrt{N}} \sum_n e^{i\mathbf{k}\cdot\mathbf{R}_n} \phi_{ta}(\mathbf{r} - \mathbf{R}_n - \boldsymbol{\tau}_a) \quad (1.52)$$

where N is the number of unit cells. The factor $e^{i\mathbf{k}\cdot\mathbf{R}_n}$ ensures that ψ is of the Bloch form.

In the tight-binding approximation, an electron wavefunction is expressed as a linear combination of the atomic orbitals of Eq. (1.52):

$$\psi_{\mathbf{k}}(\mathbf{r}) = \sum_{ta} c_{ta}(\mathbf{k}) \phi_{\mathbf{k}}^{ta}(\mathbf{r}) \quad (1.53)$$

We could now solve the Schrödinger equation, but it is more useful trying a different approach and working in second quantization.

We start with a system of free electrons. Using Eq. (1.50), working in the extended Brillouin zone scheme and dropping the band index n , we can write the Hamiltonian as

$$\hat{H}_{\text{free}} = \sum_{\mathbf{k}} \epsilon_{\mathbf{k}} \hat{c}_{\mathbf{k}}^{\dagger} \hat{c}_{\mathbf{k}} \quad (1.54)$$

where

$$\epsilon_{\mathbf{k}} = \frac{\hbar \mathbf{k}^2}{2m} \quad (1.55)$$

The creation and annihilation operators in the momentum space are related to the respective creation and annihilation operators in position space by a Fourier transformation

$$\hat{c}_{\mathbf{k}}^{\dagger} = \frac{1}{\sqrt{N}} \sum_j e^{i\mathbf{k} \cdot \mathbf{R}_j} \hat{c}_j^{\dagger} \quad (1.56)$$

$$\hat{c}_{\mathbf{k}} = \frac{1}{\sqrt{N}} \sum_j e^{-i\mathbf{k} \cdot \mathbf{R}_j} \hat{c}_j \quad (1.57)$$

Using Eqs. (1.56) and (1.57) we can write the Hamiltonian in position space

$$\hat{H}_{\text{free}} = \frac{1}{N} \sum_{ij} \sum_{\mathbf{k}} \epsilon_{\mathbf{k}} e^{i\mathbf{k} \cdot (\mathbf{R}_i - \mathbf{R}_j)} \hat{c}_i^{\dagger} \hat{c}_j \quad (1.58)$$

where N is the number of available \mathbf{k} states. It is easy to interpret the effect of the creation and annihilation operators in Eq. (1.58): an electron moves from \mathbf{R}_j to \mathbf{R}_i and

$$\tilde{t}_{ij} = \sum_{\mathbf{k}} \epsilon_{\mathbf{k}} e^{i\mathbf{k} \cdot (\mathbf{R}_i - \mathbf{R}_j)} \quad (1.59)$$

is the associated energy.

If we now consider a system of non-interacting electrons moving in a Bravais lattice, so subject to a periodic ionic potential, the dispersion relation in Eq. (1.55) will change, and the factor \tilde{t}_{ij} will change too. We will refer to the new factor t_{ij} as the *hopping parameter*. It can be interpreted as the change in energy after an electron moves from the site j to the site i . The result is that the electrons will tend to become more localized,

since the value of t_{ij} will be very small for large distances $|\mathbf{R}_i - \mathbf{R}_j|$. In the tight-binding approximation, we assume

$$t_{ij} = \begin{cases} -t & \text{for nearest neighbors} \\ 0 & \text{otherwise} \end{cases} \quad (1.60)$$

The tight-binding Hamiltonian becomes

$$\hat{H}_{tb} = -t \sum_{\langle i,j \rangle} (\hat{c}_i^\dagger \hat{c}_j + \hat{c}_j^\dagger \hat{c}_i) \quad (1.61)$$

where $\langle i,j \rangle$ means that the sum is extended only over the (i,j) that are nearest neighbours.

It is useful to express Eq. (1.61) in the momentum-space representation. In order to do so, we rewrite Eq. (1.61) as

$$\hat{H}_{tb} = -t \sum_{\langle i,j \rangle} (\hat{c}_i^\dagger \hat{c}_j + \hat{c}_j^\dagger \hat{c}_i) = -\frac{t}{2} \sum_i \sum_\delta (\hat{c}_i^\dagger \hat{c}_{i+\delta} + \hat{c}_{i+\delta}^\dagger \hat{c}_i) \quad (1.62)$$

where the sum over δ is carried over all the nearest neighbours of the site i and the factor $1/2$ is inserted to avoid double counting. Using Eqs. (1.56) and (1.57), we can express the Hamiltonian in the momentum-space representation:

$$\begin{aligned} \hat{H}_{tb} &= -\frac{t}{2} \frac{1}{N} \sum_i \sum_\delta \sum_{\mathbf{k}, \mathbf{k}'} (e^{-i\mathbf{k} \cdot \mathbf{R}_i} e^{i\mathbf{k}' \cdot (\mathbf{R}_i + \mathbf{R}_\delta)} \hat{c}_\mathbf{k}^\dagger \hat{c}_{\mathbf{k}'} + e^{i\mathbf{k} \cdot \mathbf{R}_i} e^{-i\mathbf{k}' \cdot (\mathbf{R}_i + \mathbf{R}_\delta)} \hat{c}_\mathbf{k}^\dagger \hat{c}_{\mathbf{k}'}) \\ &= -\frac{t}{2} \sum_{\mathbf{k}, \delta} (e^{i\mathbf{k} \cdot \mathbf{R}_\delta} + e^{-i\mathbf{k} \cdot \mathbf{R}_\delta}) \hat{c}_\mathbf{k}^\dagger \hat{c}_\mathbf{k} = -t \sum_{\mathbf{k}, \delta} \cos(\mathbf{k} \cdot \mathbf{R}_\delta) \hat{c}_\mathbf{k}^\dagger \hat{c}_\mathbf{k} \quad (1.63) \end{aligned}$$

which can be written as

$$\hat{H}_{tb} = \sum_{\mathbf{k}} \epsilon_{\mathbf{k}}^{tb} \hat{c}_\mathbf{k}^\dagger \hat{c}_\mathbf{k} \quad (1.64)$$

with

$$\epsilon_{\mathbf{k}}^{tb} = -t \sum_\delta \cos(\mathbf{k} \cdot \mathbf{R}_\delta) \quad (1.65)$$

1.2.4 Phonons

So far, we have treated the crystal as a collection of ions fixed in a lattice and non-interacting electrons. However, the ions are not really fixed. The crystal is held together by the bonds between the atoms. If we suppose the potential of the bonding force between two ions i and j to be $v_{I-I}(|\mathbf{R}_i - \mathbf{R}_j|)$, we can write the total potential as

$$V_{I-I}(\mathbf{R}_1, \mathbf{R}_2, \dots) = \frac{1}{2} \sum_{ij} v_{I-I}(|\mathbf{R}_i - \mathbf{R}_j|) \quad (1.66)$$

where the sum is extended over all the ions, and we have implicitly assumed that the potential is dependent only on the distance between the ions. The positions of the ions in the lattice

$$\mathbf{R}_n^a = \mathbf{R}_n + \boldsymbol{\tau}_a \quad (1.67)$$

are now interpreted as the equilibrium positions of the potential (1.66), whereas the actual positions are given by

$$\mathbf{R}_n^a(t) = \mathbf{R}_n^a + \delta \mathbf{R}_n^a(t) = \mathbf{R}_n^a + \boldsymbol{\xi}_{n,a}(t) \quad (1.68)$$

Expanding (1.66) in a Taylor series up to the second order, we can treat the system in the harmonic approximation.

$$V_{I-I}(\mathbf{R}_1, \mathbf{R}_2, \dots) \simeq \frac{1}{2} \sum_{\alpha\alpha'} \sum_{m m'} \frac{\partial^2 V_{I-I}}{\partial \xi_m^\alpha \partial \xi_{m'}^{\alpha'}} \xi_m^\alpha \xi_{m'}^{\alpha'} \quad (1.69)$$

where $\alpha = (x, y, z)$ and $m = (n, a)$. In this form, the Hamiltonian

$$H_{I-I}(\mathbf{R}_1, \mathbf{R}_2, \dots) = \sum_{n,a} \frac{(\mathbf{p}_n^a)^2}{2m_a} + V_{I-I}(\mathbf{R}_1, \mathbf{R}_2, \dots) \quad (1.70)$$

is not separable. Making a canonical change of coordinate from the position space to the reciprocal space, we can decouple the Hamiltonian into a sum of non-interacting Hamiltonians

$$H_{I-I} = \sum_{\mathbf{q}} H_{\mathbf{q}} \quad (1.71)$$

where \mathbf{q} is a vector in the reciprocal space. A detailed analysis shows that the final Hamiltonian for a crystal with r atoms per unit cell in d dimensions, expressed in second quantization is

$$\hat{H}_{ph} = \sum_{\lambda \mathbf{q}} \hbar \omega_{\lambda \mathbf{q}} \left(\hat{b}_{\lambda \mathbf{q}}^\dagger \hat{b}_{\lambda \mathbf{q}} + \frac{1}{2} \right) \quad (1.72)$$

where \mathbf{q} is a wavevector, $\lambda = (0, 1, \dots, rd)$ a branch index, ω eigenfrequencies and \hat{b}^\dagger and \hat{b} creation and annihilation operators. Thus, the vibrational modes can be interpreted as a collection of bosonic quasi-particles of momentum \mathbf{q} and frequency $\omega_{\lambda \mathbf{q}}$. We call these quasi-particles phonons.

The system has a non-zero energy ground state

$$E_0 = \sum_{\lambda \mathbf{q}} \frac{1}{2} \hbar \omega_{\lambda \mathbf{q}} \quad (1.73)$$

The relation between the displacement and the creation and annihilation operators is

$$\delta \mathbf{R}_n^a = \sum_{\mathbf{q} \lambda} A_{\mathbf{q} \lambda}^a \hat{e}_{\mathbf{q} \lambda}^a e^{i \mathbf{q} \cdot \mathbf{R}_n^a} (\hat{b}_{\mathbf{q} \lambda} + \hat{b}_{-\mathbf{q} \lambda}^\dagger) \quad (1.74)$$

where $\hat{e}_{q\lambda}^a$ is the polarization vector and

$$A_{q\lambda}^a = \sqrt{\frac{\hbar}{2M_a N \omega_{q\lambda}}} \quad (1.75)$$

where M_a is mass of the a^{th} atom and N the number of atoms. The polarization vector $\hat{e}_{q\lambda}^a$ is used to describe the direction of the displacement δR_n^a with respect to the direction of propagation q . We have transversal phonons if $q \cdot \hat{e}_{q\lambda}^a = 0$ and longitudinal phonons if $q \times \hat{e}_{q\lambda}^a = 0$

To generalize, we have considered a Hamiltonian

$$\hat{H} = \sum_i \hat{H}_i(\mathbf{r}_i, \mathbf{p}_i) + \sum_{ij} \hat{H}_{ij}(\mathbf{r}_i, \mathbf{p}_i, \mathbf{r}_j, \mathbf{p}_j) \quad (1.76)$$

and after a canonical change of coordinates, we have transformed it in

$$\hat{H} = E_0 + \sum_q E_q \hat{c}_q^\dagger \hat{c}_q + \Delta E \quad (1.77)$$

The first term, E_0 is the ground state energy, the second describe a system of non-interacting particles and the third is a residual energy. This method is valid as long as $\Delta E_q \ll E_q$. In the case of phonons, $\Delta E = 0$ because we made a harmonic approximation. The non-harmonic terms would describe the interaction between phonons, which would result in $\Delta E \neq 0$ [18].

1.2.5 Electron-phonon interaction

Now that we have described electrons and phonons, we can investigate how they interact with each other [18, 19]. Their interaction is of vital importance in solid state physics, polarons included. Our discussion starts with a periodic potential

$$V(\mathbf{r}, t) = \sum_{l,a} V_a(\mathbf{r} - \mathbf{R}_l^a(t)) \quad (1.78)$$

perturbed from its equilibrium position. l is an index of lattice points and a of ions in the unit cell. $\mathbf{R}_l^a(t)$ is the position of the ion, and it is given by Eq. (1.68):

$$\mathbf{R}_l^a(t) = \mathbf{R}_l^a + \delta \mathbf{R}_l^a(t) \quad (1.79)$$

For typical vibrations, it can be shown that the displacements $\xi = |\delta \mathbf{R}_l^a(t)|$ are much smaller than the atomic spacing d . In particular

$$\frac{\xi}{d} \simeq \left[\frac{m}{M} \right]^{\frac{1}{4}} \quad (1.80)$$

and the phonon energy E_{ph} scales as

$$\frac{E_{\text{ph}}}{E_{\text{el}}} \simeq \left(\frac{m}{M}\right)^{\frac{1}{2}} \quad (1.81)$$

where E_{el} is the electron energy, m the electron mass and M the atomic mass. Given this scaling considerations, we can assume the general band structure of the crystal not to be modified. However, the interaction with the phonons can slightly modify it. This results in a modification of the electron effective mass, of the order of the phonon energies.

Using the assumption of small displacements, we can expand the potential in Eq. (1.78) in a Taylor series.

$$V(\mathbf{r}, t) = \sum_{l,a} V_a(\mathbf{r} - \mathbf{R}_l^a - \delta \mathbf{R}_l^a(t)) \simeq \sum_{l,a} [V_a(\mathbf{r} - \mathbf{R}_l^a) + \delta \mathbf{R}_l^a(t) \cdot \nabla_{\mathbf{r}} V_a(\mathbf{r} - \mathbf{R}_l^a)] \quad (1.82)$$

Terms of higher orders take into account anharmonic oscillations, which were already neglected in the study of the phonon Hamiltonian. The term $V_a(\mathbf{r} - \mathbf{R}_l^a)$ does not depend on the deviation of the ions from their equilibrium positions. In fact, it is exactly the static periodic potential considered in the study of electrons in Section 1.2.2.

The total Hamiltonian of the system can be written as the sum of three terms

$$\hat{H} = \hat{H}_{\text{el}} + \hat{H}_{\text{ph}} + \hat{H}_{\text{el-ph}} \quad (1.83)$$

where \hat{H}_{el} and \hat{H}_{ph} are respectively the electrons and phonons Hamiltonians, given by Eq. (1.50) and Eq. (1.72). The last term describes the electron-phonon contribution, and it can be identified with

$$\hat{H}_{\text{el-ph}} = \sum_{l,a} \delta \mathbf{R}_l^a(t) \cdot \nabla_{\mathbf{r}} V_a(\mathbf{r} - \mathbf{R}_l^a) \quad (1.84)$$

We can use Eq. (1.74) to rewrite it expanding the displacements in phonon coordinates

$$\hat{H}_{\text{el-ph}} = \sum_a \sum_{\mathbf{q}\lambda} A_{\mathbf{q}\lambda}^a \hat{\epsilon}_{\mathbf{q}\lambda}^a \cdot \left(\sum_l e^{i\mathbf{q} \cdot \mathbf{R}_l^a} \cdot \nabla_{\mathbf{r}} V_a(\mathbf{r} - \mathbf{R}_l^a) \right) (\hat{b}_{\mathbf{q}\lambda} + \hat{b}_{-\mathbf{q}\lambda}^\dagger) \quad (1.85)$$

where $A_{\mathbf{q}\lambda}^a$ is given by Eq. (1.75), $\hat{\epsilon}_{\mathbf{q}\lambda}^a$ is the polarization vector, \mathbf{q} the momentum of the phonon and $\hat{b}_{-\mathbf{q}\lambda}^\dagger$ and $\hat{b}_{\mathbf{q}\lambda}$ are the phonon creation and annihilation operators.

The electron part of the previous expression is still written in the language of first quantization. Using Eq. (1.36), we can express it in a second-quantized form. Suppressing the band indices and using the extended zone scheme, so that \mathbf{k}' and \mathbf{k} are not limited to the first Brillouin zone,

$$\hat{H}_{\text{el-ph}} = \sum_{\mathbf{k}'\mathbf{k}} \langle \mathbf{k}' | \hat{H}_{\text{el-ph}} | \mathbf{k} \rangle \hat{c}_{\mathbf{k}'}^\dagger \hat{c}_{\mathbf{k}} = \sum_{\mathbf{k}'\mathbf{k}} \sum_{\mathbf{q}\lambda} M_{\mathbf{k}'\rightarrow\mathbf{k}}^\lambda(\mathbf{q}) \hat{c}_{\mathbf{k}'}^\dagger \hat{c}_{\mathbf{k}} (\hat{b}_{\mathbf{q}\lambda} + \hat{b}_{-\mathbf{q}\lambda}^\dagger) \quad (1.86)$$

where the electron-phonon matrix M can be derived from Eq. (1.85). The previous expression can be interpreted as the transition of an electron from the state $|\mathbf{k}\rangle$ to the state $|\mathbf{k}'\rangle$ with either the creation of a phonon of momentum $-\mathbf{q}$ or the annihilation of a phonon of momentum \mathbf{q} . The matrix element $M_{\mathbf{k} \rightarrow \mathbf{k}'}^{\lambda}(\mathbf{q})$ gives the mechanical amplitude of such a process.

In order to evaluate M , we need to compute $\langle \mathbf{k}' | \hat{H}_{\text{el-ph}} | \mathbf{k} \rangle$. We start with a Fourier transform of the potential

$$V(\mathbf{r}) = \sum_{\mathbf{q}} V_a(\mathbf{q}) e^{i\mathbf{q} \cdot \mathbf{r}} \quad (1.87)$$

where V_a is the atomic form factor, and it is given by

$$V_a(\mathbf{q}) = \frac{1}{\Omega_a} \int e^{-i\mathbf{q} \cdot \mathbf{r}} V_a(\mathbf{r}) d\mathbf{r} = \frac{wN}{\Omega} \int e^{-i\mathbf{q} \cdot \mathbf{r}} V_a(\mathbf{r}) d\mathbf{r} \quad (1.88)$$

where Ω_a is the volume of a unit cell, Ω the volume of the crystal, N the number of unit cells and w the number of atoms per unit cell. We compute the gradient of the potential $\nabla_{\mathbf{r}} V_a(\mathbf{r})$ expressed as a Fourier series, and we evaluate it at $\mathbf{r} - \mathbf{R}_l^a$:

$$\nabla_{\mathbf{r}} V_a(\mathbf{r} - \mathbf{R}_l^a) = \frac{i}{wN} \sum_{\mathbf{q}'} \mathbf{q}' e^{i\mathbf{q}' \cdot \mathbf{r}} V_a(\mathbf{r}) e^{-i\mathbf{q}' \cdot \mathbf{R}_l^a} \quad (1.89)$$

Equation (1.85) can now be rewritten using Eq. (1.89) as

$$\hat{H}_{\text{el-ph}} = \frac{i}{wN} \sum_{l a \lambda} \sum_{\mathbf{q} \mathbf{q}'} A_{\mathbf{q} \lambda}^a \hat{\epsilon}_{\mathbf{q} \lambda}^a \cdot \mathbf{q}' e^{i\mathbf{q}' \cdot \mathbf{r}} e^{i(\mathbf{q}-\mathbf{q}') \cdot \mathbf{R}_l^a} V_a(\mathbf{q}') (\hat{b}_{\mathbf{q} \lambda} + \hat{b}_{-\mathbf{q} \lambda}^\dagger) \quad (1.90)$$

We know that

$$\sum_l e^{i(\mathbf{q}-\mathbf{q}') \cdot \mathbf{R}_l^a} = N \delta(\mathbf{q} - \mathbf{q}' + \mathbf{G}) \quad (1.91)$$

where \mathbf{G} is a vector of the reciprocal lattice. Then, most of the terms of the previous expression are zero, and we obtain

$$\begin{aligned} & \langle \mathbf{k}' | \hat{H}_{\text{el-ph}} | \mathbf{k} \rangle \\ &= \frac{i}{w} \sum_{a \lambda \mathbf{q}} A_{\mathbf{q} \lambda}^a \sum_{\mathbf{G}} e^{-i\mathbf{G} \cdot \mathbf{r}_a} V_a(\mathbf{q} + \mathbf{G}) \hat{\epsilon}_{\mathbf{q} \lambda}^a \cdot (\mathbf{q} + \mathbf{G}) (\hat{b}_{\mathbf{q} \lambda} + \hat{b}_{-\mathbf{q} \lambda}^\dagger) \langle \mathbf{k}' | e^{i(\mathbf{q} + \mathbf{G}) \cdot \mathbf{r}} | \mathbf{k} \rangle \end{aligned} \quad (1.92)$$

where we have used that $\mathbf{G} \cdot \mathbf{R}_l = 2\pi n$, with n integer, to simplify the sum over l . Finally, inserting this result in Eq. (1.86), we obtain an expression for the matrix element

$$M_{\mathbf{k} \rightarrow \mathbf{k}'}^{\lambda}(\mathbf{q}) = \frac{i}{w} \sum_{a \mathbf{G}} \sqrt{\frac{\hbar}{2M_a N \omega_{\mathbf{q} \lambda}}} e^{-i\mathbf{G} \cdot \mathbf{r}_a} V_a(\mathbf{q} + \mathbf{G}) \hat{\epsilon}_{\mathbf{q} \lambda}^a \cdot (\mathbf{q} + \mathbf{G}) \langle \mathbf{k}' | e^{i(\mathbf{q} + \mathbf{G}) \cdot \mathbf{r}} | \mathbf{k} \rangle \quad (1.93)$$

We can compute the matrix element for a simple case where the initial and final state of the electron are plane waves. In this case,

$$\langle \mathbf{k}' | e^{i(\mathbf{q} + \mathbf{G}) \cdot \mathbf{r}} | \mathbf{k} \rangle = \delta_{\mathbf{k}', \mathbf{k} + \mathbf{q} + \mathbf{G}} \quad (1.94)$$

and

$$M_{\mathbf{k} \rightarrow \mathbf{k}'}^{\lambda}(\mathbf{q}) = \frac{i}{w} \sum_{aG} \sqrt{\frac{\hbar}{2M_a N \omega_{q\lambda}}} e^{-i\mathbf{G} \cdot \boldsymbol{\tau}_a} V_a(\mathbf{q} + \mathbf{G}) \hat{\epsilon}_{q\lambda}^a \cdot (\mathbf{q} + \mathbf{G}) \delta_{\mathbf{k}', \mathbf{k} + \mathbf{q} + \mathbf{G}} \quad (1.95)$$

The scattering process that we have explained earlier is now more clear. An electron of momentum $\hbar\mathbf{k}$ is scattered in an electron of momentum $\hbar(\mathbf{k} + \mathbf{q} + \mathbf{G})$ by the emission of a phonon of momentum $-\mathbf{q}$ or the absorption of a phonon of momentum \mathbf{q} . We can identify two processes: the normal (N) process, where $\mathbf{G} = 0$, and the umklapp (U) process, where $\mathbf{G} \neq 0$. In the normal process $\mathbf{k}' = \mathbf{k} + \mathbf{q}$, assuming $w = 1$,

$$M_{\mathbf{k} \rightarrow \mathbf{k} + \mathbf{q}}^{\lambda}(\mathbf{q}) = i \sqrt{\frac{\hbar}{2M_a N \omega_{q\lambda}}} V_a(\mathbf{q}) \hat{\epsilon}_{q\lambda} \cdot \mathbf{q} \quad (1.96)$$

It is clear that in this type of process, only longitudinal phonons contribute to the scattering, since for transversal phonons $\hat{\epsilon}_{q\lambda} \cdot \mathbf{q} = 0$.

The electrons are affected by deformations of the lattice in several ways [20]. The main effects of the coupling between electrons and phonons are:

- the scattering of electrons from a state \mathbf{k} to a state \mathbf{k}' , resulting in electrical resistivity;
- the absorption or creation of phonons;
- the creation of an attractive force between electrons, which is essential to explain superconductivity.

Another consequence is that electrons, moving in the lattice, carry a lattice polarization field with them. The particle resulting from the combination of the electron and the polarization field is called *polaron*, and it has a larger effective mass than the electron alone. In the next chapter, and in the rest of the thesis, we will focus on this last type of interaction.

2

THE POLARON PROBLEM

In this chapter we will derive and compare different models that are used to describe polarons. We will start with the Landau-Pekar model, the first to be proposed and the simplest one. Then, Fröhlich and Holstein models will be discussed. These two models are the ones currently used to describe respectively large and small polarons. A comparison of these two types of polarons is made in the last section.

2.1 LANDAU-PEKAR MODEL

In the Landau-Pekar model, the electron is described by a wavefunction $\Psi(\mathbf{r})$ moving in a dielectric continuum medium. The static potential of the crystal is taken into account associating at the electron an effective mass m^* (see Section 1.2.2). If we allow the medium to be polarized, the energy of the system is given by the kinetic energy of electron plus the energy of the electromagnetic field

$$E = \frac{\hbar^2}{2m^*} \int d\mathbf{r} |\nabla \Psi(\mathbf{r})|^2 + \frac{1}{2} \int d\mathbf{r} \mathbf{E} \cdot \mathbf{D} \quad (2.1)$$

\mathbf{D} can be expressed, using the Gauss law, as $\nabla \cdot \mathbf{D} = \rho = -e|\Psi(\mathbf{r})|^2$, or equivalently

$$\mathbf{D} = -\frac{e}{4\pi} \nabla \int d\mathbf{r}' \frac{|\Psi(\mathbf{r}')|^2}{|\mathbf{r} - \mathbf{r}'|} \quad (2.2)$$

Remembering that for a dielectric medium $\mathbf{D} = \epsilon_0 \epsilon^0 \mathbf{E}$, where ϵ_0 is the vacuum permittivity and ϵ^0 is the static dielectric constant, we obtain for the electrostatic energy

$$\frac{1}{2} \int d\mathbf{r} \mathbf{E} \cdot \mathbf{D} = \frac{1}{2} \frac{1}{4\pi\epsilon_0} \frac{e^2}{\epsilon^0} \int d\mathbf{r} d\mathbf{r}' \frac{|\Psi(\mathbf{r})|^2 |\Psi(\mathbf{r}')|^2}{|\mathbf{r} - \mathbf{r}'|} \quad (2.3)$$

In the previous expression, \mathbf{E} includes contributions from both the displacement of the ions and the electric screening of the electrons. The latter effect is already taken into account by the effective mass in the expression of the kinetic energy, so we have to remove its contribution. Since the ions have a much larger mass than the electrons, they will not contribute to the high-frequency dielectric constant ϵ^∞ . Thus, ϵ^∞ expresses the contribution of electrons to the total dielectric constant. Subtracting it in the previous expression, we obtain

$$\frac{1}{2} \int d\mathbf{r} \mathbf{E} \cdot \mathbf{D} = \frac{1}{2} \frac{e^2}{4\pi\epsilon_0} \left(\frac{1}{\epsilon^0} - \frac{1}{\epsilon^\infty} \right) \int d\mathbf{r} d\mathbf{r}' \frac{|\Psi(\mathbf{r})|^2 |\Psi(\mathbf{r}')|^2}{|\mathbf{r} - \mathbf{r}'|} \quad (2.4)$$

If we define $1/\kappa = 1/\epsilon^\infty - 1/\epsilon^0$, we can rewrite the total energy as a functional of ψ

$$E[\psi] = \frac{\hbar^2}{2m^*} \int d\mathbf{r} |\nabla \psi(\mathbf{r})|^2 - \frac{1}{2} \frac{e^2}{4\pi\epsilon_0} \frac{1}{\kappa} \int d\mathbf{r} d\mathbf{r}' \frac{|\psi(\mathbf{r})|^2 |\psi(\mathbf{r}')|^2}{|\mathbf{r} - \mathbf{r}'|} \quad (2.5)$$

Following a variational approach, this functional can be minimized to find the polaron ground state energy. To do so, we must include a normalization constraint. This is done with the help of a Lagrange multiplier ε

$$\begin{aligned} E[\psi, \varepsilon] = & \frac{\hbar^2}{2m^*} \int d\mathbf{r} |\nabla \psi(\mathbf{r})|^2 - \frac{1}{2} \frac{e^2}{4\pi\epsilon_0} \frac{1}{\kappa} \int d\mathbf{r}' \frac{|\psi(\mathbf{r})|^2 |\psi(\mathbf{r}')|^2}{|\mathbf{r} - \mathbf{r}'|} \\ & - \varepsilon \left(\int d\mathbf{r} |\psi(\mathbf{r})|^2 - 1 \right) \end{aligned} \quad (2.6)$$

Minimizing with respect to ψ^* and ε , we obtain a Schrödinger-type equation

$$\left(-\frac{\hbar^2}{2m^*} \nabla^2 - \frac{e^2}{4\pi\epsilon_0} \frac{1}{\kappa} \int d\mathbf{r}' \frac{|\psi(\mathbf{r}')|^2}{|\mathbf{r} - \mathbf{r}'|} \right) \psi(\mathbf{r}) = \varepsilon \psi(\mathbf{r}) \quad (2.7)$$

The Lagrange multiplier ε has the dimension of an energy, but it is not exactly the polaron ground state energy. Projecting Eq. (2.7) onto ψ^* and confronting the result with Eq. (2.6), we obtain the ground state energy E_0

$$E_0 = \varepsilon + \frac{1}{2} \frac{e^2}{4\pi\epsilon_0} \frac{1}{\kappa} \int d\mathbf{r}' \frac{|\psi(\mathbf{r})|^2 |\psi(\mathbf{r}')|^2}{|\mathbf{r} - \mathbf{r}'|} \quad (2.8)$$

Equation (2.7) is not known to have an exact solution. However, given the similarity with the hydrogen atom Hamiltonian, we can use as a trial wavefunction $(\pi r_p^3)^{-1/2} e^{-r/r_p}$ and minimize E with respect to r_p . As in the hydrogen atom, the kinetic term minimization favours larger r_p (delocalized states) and the potential term favours smaller r_p (localized states). Performing the minimization [21], r_p is found to be

$$r_p = \frac{16}{5} \frac{\kappa}{m^*/m_e} a_0 \quad (2.9)$$

where m_e is the mass of the electron and a_0 the Bohr radius. The value of the ground state energy is

$$E_0 = -\frac{50}{512} \alpha^2 \hbar \omega_{LO} \quad (2.10)$$

where ω_{LO} is the characteristic frequency of longitudinal optical phonon and

$$\alpha = \frac{e^2}{4\pi\epsilon_0 \hbar} \sqrt{\frac{m^*}{2\hbar\omega_{LO}}} \frac{1}{\kappa} \quad (2.11)$$

Despite its simplicity, the Landau-Pekar model provides simple formulas for the polaron ground state, radius and effective mass [4]. However, to have polaron bound

states, κ must be positive, which implies $\epsilon^0 > \epsilon^\infty$. This is true only for polar crystals, but polarons are observed in non-polar crystals as well. Moreover, this model carries an intrinsic contradiction. Treating the medium as a continuum requires the polaron to be large, but formally justified results can only be obtained in the strong coupling regime, a situation improbable for real materials.

2.2 FRÖHLICH POLARONS

We have anticipated in Section 2.1 a simple model for polarons. We are now ready to improve that first simple model, taking now into account a more precise mechanics of the lattice polarization. In this section we will discuss the Fröhlich Hamiltonian, derived by Fröhlich in 1950 [5]. This Hamiltonian is appropriate to describe polarons in ionic crystals and polar semiconductors. In these materials we expect electrons to interact strongly with longitudinal optical phonons through the electric field produced by the polarization of the lattice. The contribution of transversal phonons is expected to be negligible because of the smaller electric field they produce.

2.2.1 Derivation of the Fröhlich Hamiltonian

In this section we derive the Fröhlich Hamiltonian following the approach described by Kittel [20]. We assume the longitudinal phonons to be dispersionless (with frequency ω_{LO}) and we treat the polarizable medium as a continuum.

In an ionic crystal, the polarization \mathbf{P} can be considered as the sum of two components: the optical polarization \mathbf{P}_o and the infra-red polarization \mathbf{P}_{ir} . The former is due to the displacement of bound electrons, and it is characterized by a resonance frequency in the optical or ultraviolet region; the latter is due to the displacement of ions and its resonance frequency is in the infra-red region. Given the slow velocities of the electrons that we are going to consider, the optical polarization is always excited at its static value. Thus, given the absence of a dependence on the velocity of the electron, the optical polarization \mathbf{P}_o is of no interest to us, since it does not modify the energy of the electron between different states. On the other hand, this does not apply to the infra-red polarization, because of its lower resonance frequency. At long distances from the electric charge (placed at \mathbf{r}_0), \mathbf{P}_{ir} can be obtained subtracting the optical polarization \mathbf{P}_o from the total polarization \mathbf{P} . Thus, it can be derived from an electric potential $V(\mathbf{r})$ by

$$4\pi\mathbf{P}_{\text{ir}}(\mathbf{r}) = \nabla V(\mathbf{r}) \quad (2.12)$$

where

$$V(\mathbf{r}) = -\frac{1}{\kappa} \frac{e}{|\mathbf{r} - \mathbf{r}_0|} \quad (2.13)$$

with $1/\kappa = 1/\epsilon^\infty - 1/\epsilon^0$. As in the Landau-Pekar model, the contribution of the lattice to the dielectric constant (κ) is obtained by removing the contribution of the electrons (ϵ^∞) from the static dielectric constant (ϵ^0).

The infra-red polarization is proportional to the amplitude of the displacement of the ions. Generalizing Eq. (1.74) for a generic point \mathbf{r} , we can express the displacement in the point \mathbf{r} as

$$\xi(\mathbf{r}) = \sum_{\mathbf{q}} A \hat{\epsilon}_{\mathbf{q}} e^{i\mathbf{q} \cdot \mathbf{r}} (\hat{b}_{\mathbf{q}} + \hat{b}_{-\mathbf{q}}^\dagger) \quad (2.14)$$

where we have dropped the indices a and λ because we are considering atoms of the same mass and phonons of the same branch. Moreover, A does not depend on \mathbf{q} because the phonons are assumed to be dispersionless. Since we are considering only longitudinal phonons, the polarization vector $\hat{\epsilon}_{\mathbf{q}}$ must be parallel to \mathbf{q} . However, we cannot simply suppose $\hat{\epsilon}_{\mathbf{q}} = \hat{q}$. In fact, we have to guarantee that $\xi(\mathbf{r})$ is real:

$$\xi^\dagger(\mathbf{r}) = \sum_{\mathbf{q}} A \hat{\epsilon}_{\mathbf{q}}^\dagger e^{-i\mathbf{q} \cdot \mathbf{r}} (\hat{b}_{\mathbf{q}}^\dagger + \hat{b}_{-\mathbf{q}}) = \sum_{\mathbf{q}} A \hat{\epsilon}_{-\mathbf{q}}^\dagger e^{i\mathbf{q} \cdot \mathbf{r}} (\hat{b}_{\mathbf{q}} + \hat{b}_{-\mathbf{q}}^\dagger) = \xi(\mathbf{r}) \quad (2.15)$$

This implies $\hat{\epsilon}_{\mathbf{q}}^\dagger = \hat{\epsilon}_{-\mathbf{q}}$, and then $\hat{\epsilon}_{\mathbf{q}} = i\hat{q}$.

As we anticipated, P_{ir} is proportional to the amplitude of the displacement

$$P_{ir} = F \xi(\mathbf{r}) = iF \sum_{\mathbf{q}} A \hat{q} e^{i\mathbf{q} \cdot \mathbf{r}} (\hat{b}_{\mathbf{q}} + \hat{b}_{-\mathbf{q}}^\dagger) \quad (2.16)$$

where F is a constant to be determined. We expand the electric potential in a Fourier series

$$V(\mathbf{r}) = \sum_{\mathbf{q}} V(\mathbf{q}) e^{i\mathbf{q} \cdot \mathbf{r}} \quad (2.17)$$

and we compute the gradient

$$\nabla V(\mathbf{r}) = i \sum_{\mathbf{q}} \mathbf{q} V(\mathbf{q}) e^{i\mathbf{q} \cdot \mathbf{r}} \quad (2.18)$$

Using Eq. (2.12) and comparing Eq. (2.16) with Eq. (2.18), we find

$$V(\mathbf{q}) = 4\pi \frac{FA}{q} (\hat{b}_{\mathbf{q}} + \hat{b}_{-\mathbf{q}}^\dagger) \quad (2.19)$$

We now want to express the constant F in terms of the interaction energy of two electrons in a polarizable material of dielectric constant ϵ . We consider two electrons completely localized in two points \mathbf{r}_1 and \mathbf{r}_2 . The electrons will interact directly through the vacuum electric field and indirectly through a perturbation induced by the

optical phonon field. The interaction Hamiltonian is given by the sum of the potential of the two electrons

$$\begin{aligned} H_{\text{el-el}} &= -eV(\mathbf{r}_1) - eV(\mathbf{r}_2) = 4\pi eFA \sum_{\mathbf{q}} \mathbf{q}^{-1} (e^{i\mathbf{q}\cdot\mathbf{r}_1} + e^{i\mathbf{q}\cdot\mathbf{r}_2})(\hat{b}_{\mathbf{q}} + \hat{b}_{-\mathbf{q}}^\dagger) \\ &= 4\pi eFA \sum_{\mathbf{q}} \mathbf{q}^{-1} \left[\hat{b}_{\mathbf{q}}(e^{i\mathbf{q}\cdot\mathbf{r}_1} + e^{i\mathbf{q}\cdot\mathbf{r}_2}) + \hat{b}_{\mathbf{q}}^\dagger(e^{-i\mathbf{q}\cdot\mathbf{r}_1} + e^{-i\mathbf{q}\cdot\mathbf{r}_2}) \right] \quad (2.20) \end{aligned}$$

where in the second line we have changed the sign of \mathbf{q} in the second term, using the fact that the sum is extended over all \mathbf{q} . The second-order energy perturbation caused by the previous Hamiltonian is given by

$$\Delta E = - \sum_{\mathbf{q}} \frac{\langle 0 | H_{\text{el-el}} | \mathbf{q} \rangle \langle \mathbf{q} | H_{\text{el-el}} | 0 \rangle}{\hbar\omega_{\text{LO}}} \quad (2.21)$$

where $|0\rangle$ and $|\mathbf{q}\rangle$ are respectively states with no phonons and a single LO phonon in the state \mathbf{q} with energy $\hbar\omega_{\text{LO}}$. Inserting Eq. (2.20) in the previous expression and dropping the terms with \mathbf{r}_1 and \mathbf{r}_2 alone, which are self-energy terms,

$$\begin{aligned} \Delta E &= -2 \sum_{\mathbf{q}} \frac{\langle 0 | eV(\mathbf{r}_1) | \mathbf{q} \rangle \langle \mathbf{q} | eV(\mathbf{r}_2) | 0 \rangle}{\hbar\omega_{\text{LO}}} \\ &= -2 \frac{(4\pi eFA)^2}{\hbar\omega_{\text{LO}}} \sum_{\mathbf{q}} \mathbf{q}^{-2} \langle 0 | e^{i\mathbf{q}\cdot\mathbf{r}_1} (\hat{b}_{\mathbf{q}} + \hat{b}_{\mathbf{q}}^\dagger) | \mathbf{q} \rangle \langle \mathbf{q} | e^{-i\mathbf{q}\cdot\mathbf{r}_2} (\hat{b}_{\mathbf{q}} + \hat{b}_{\mathbf{q}}^\dagger) | 0 \rangle \\ &= -2 \frac{(4\pi eFA)^2}{\hbar\omega_{\text{LO}}} \sum_{\mathbf{q}} \mathbf{q}^{-2} \langle \mathbf{q} | e^{i\mathbf{q}\cdot\mathbf{r}_1} | \mathbf{q} \rangle \langle \mathbf{q} | e^{-i\mathbf{q}\cdot\mathbf{r}_2} | \mathbf{q} \rangle \\ &= -2 \frac{(4\pi eFA)^2}{\hbar\omega_{\text{LO}}} \sum_{\mathbf{q}} \frac{e^{i\mathbf{q}\cdot(\mathbf{r}_1-\mathbf{r}_2)}}{\mathbf{q}^2} \quad (2.22) \end{aligned}$$

Knowing that, when summed over all \mathbf{q} ,

$$\sum_{\mathbf{q}} \frac{4\pi}{\mathbf{q}^2} e^{i\mathbf{q}\cdot\mathbf{r}} = \Omega \frac{1}{|\mathbf{r}|} \quad (2.23)$$

where Ω is the volume of the region of interest, we can rewrite the perturbation energy as

$$\Delta E = - \frac{8\pi\Omega A^2 F^2}{\hbar\omega_{\text{LO}}} \frac{e^2}{|\mathbf{r}_1 - \mathbf{r}_2|} \quad (2.24)$$

The form of this interaction is exactly the same of an attractive Coulomb potential between two charges placed at \mathbf{r}_1 and \mathbf{r}_2 . The origin of this attraction is the polarization of the ions of the medium. Thus, the factor

$$- \frac{8\pi\Omega A^2 F^2}{\hbar\omega_{\text{LO}}} \quad (2.25)$$

gives exactly the contribution of the ions to the dielectric constant. Since the static dielectric constant ϵ^0 includes both the contribution of ions and of the electrons, and the high-frequency dielectric constant ϵ^∞ only the contribution of the electrons, we can express Eq. (2.25) as

$$\frac{1}{\epsilon^0} = \frac{1}{\epsilon^\infty} - \frac{8\pi\Omega A^2 F^2}{\hbar\omega_{\text{LO}}} \quad (2.26)$$

The electric potential is then given by

$$V(\mathbf{r}) = \sum_{\mathbf{q}} V(\mathbf{q}) e^{i\mathbf{q}\cdot\mathbf{r}} = \sum_{\mathbf{q}} \left[\frac{2\pi e^2 \hbar\omega_{\text{LO}}}{\Omega q^2} \left(\frac{1}{\epsilon^\infty} - \frac{1}{\epsilon^0} \right) \right]^{1/2} (\hat{b}_{\mathbf{q}} + \hat{b}_{-\mathbf{q}}^\dagger) e^{i\mathbf{q}\cdot\mathbf{r}} \quad (2.27)$$

and writing it in a fully second-quantized form, we find

$$\hat{H}_{\text{el-ph}} = \sum_{\mathbf{k}'\mathbf{k}} \sum_{\mathbf{q}} \left[\frac{2\pi e^2 \hbar\omega_{\text{LO}}}{\Omega q^2} \left(\frac{1}{\epsilon^\infty} - \frac{1}{\epsilon^0} \right) \right]^{1/2} \langle \mathbf{k}' | e^{i\mathbf{q}\cdot\mathbf{r}} | \mathbf{k} \rangle (\hat{b}_{\mathbf{q}\lambda} + \hat{b}_{-\mathbf{q}\lambda}^\dagger) \hat{c}_{\mathbf{k}'\lambda}^\dagger \hat{c}_{\mathbf{k}\lambda} \quad (2.28)$$

Confronting the previous expression with Eq. (1.86), we can identify the interaction matrix

$$M_{\mathbf{k}-\mathbf{q} \rightarrow \mathbf{k}} = \left[\frac{2\pi e^2 \hbar\omega_{\text{LO}}}{\Omega q^2} \left(\frac{1}{\epsilon^\infty} - \frac{1}{\epsilon^0} \right) \right]^{1/2} \quad (2.29)$$

which is more commonly written as

$$M_{\mathbf{q}} = \frac{\hbar\omega_{\text{LO}}}{|\mathbf{q}|} \left(\frac{\hbar}{2m\omega_{\text{LO}}} \right)^{1/4} \left(\frac{4\pi\alpha}{\Omega} \right)^{1/2} \quad (2.30)$$

where α is the dimensionless Fröhlich coupling constant, defined as

$$\alpha = \frac{e^2}{\hbar} \left(\frac{1}{\epsilon^\infty} - \frac{1}{\epsilon^0} \right) \sqrt{\frac{m}{2\hbar\omega_{\text{LO}}}} \quad (2.31)$$

where m is the electron band mass.

Adding the electrons and phonons contributions, and approximating the wavefunctions of the electrons to plane waves as we did in Eq. (1.94), we can write the Fröhlich Hamiltonian as

$$\begin{aligned} H_{\text{Fröhlich}} &= \sum_{\mathbf{k}} \frac{\hbar^2 \mathbf{k}^2}{2m} + \sum_{\mathbf{q}} \hbar\omega_{\text{LO}} \left(\hat{b}_{\mathbf{q}}^\dagger \hat{b}_{\mathbf{q}} + \frac{1}{2} \right) \\ &\quad + \sum_{\mathbf{k}\mathbf{q}} \frac{\hbar\omega_{\text{LO}}}{|\mathbf{q}|} \left(\frac{\hbar}{2m\omega_{\text{LO}}} \right)^{1/4} \left(\frac{4\pi\alpha}{\Omega} \right)^{1/2} \hat{c}_{\mathbf{k}}^\dagger \hat{c}_{\mathbf{k}-\mathbf{q}} (\hat{b}_{\mathbf{q}} + \hat{b}_{-\mathbf{q}}^\dagger) \end{aligned} \quad (2.32)$$

The interaction of the electrons with the lattice described by Eq. (2.32) has multiple effects. Some consequences we may expect are:

- The electron band energy is decreased, because part of the energy is used to produce phonons.
- The effective mass of the electron is increased, because the electron has to deform the lattice while moving, carrying the deformation with itself.
- The mobility of the electron is modified, because the polaron experiences scattering effects different from the ones of a free electron.

We can analyse quantitatively the first of these two effects using approximation techniques. We will do it in the next two sections, applying perturbation theory and variational methods to the Fröhlich Hamiltonian.

2.2.2 Weak coupling limit

Polarons are often divided in two classes: large and small. The name is due to their effective radius l_p , which is defined as the effective radius of the polarized area. If l_p is greater than the interatomic distance d , the polaron is said to be large; on the contrary, if $l_p \lesssim d$, the polaron is said to be small. In the former case, the coupling is usually weak ($\alpha < 1$), in the latter it is strong ($\alpha > 1$). In the weak-coupling regime, it is possible to use perturbation theory to derive some properties of large polarons.

The total Hamiltonian is

$$\begin{aligned}\hat{H} &= \hat{H}_{\text{el}} + \hat{H}_{\text{ph}} + \hat{H}_{\text{el-ph}} \\ &= \sum_{\mathbf{k}} \frac{\hbar^2 \mathbf{k}^2}{2m} + \sum_{\mathbf{q}} \hbar \omega_{\text{LO}} \left(\hat{b}_{\mathbf{q}}^\dagger \hat{b}_{\mathbf{q}} + \frac{1}{2} \right) + \sum_{\mathbf{k}, \mathbf{q}} M_{\mathbf{q}} \hat{c}_{\mathbf{k}}^\dagger \hat{c}_{\mathbf{k}-\mathbf{q}} (\hat{b}_{\mathbf{q}} + \hat{b}_{-\mathbf{q}}^\dagger)\end{aligned}\quad (2.33)$$

where $M_{\mathbf{q}}$ is given by Eq. (2.30)

$$M_{\mathbf{q}} = \frac{\hbar \omega_{\text{LO}}}{|\mathbf{q}|} \left(\frac{\hbar}{2m \omega_{\text{LO}}} \right)^{1/4} \left(\frac{4\pi\alpha}{\Omega} \right)^{1/2} \quad (2.34)$$

and it is supposed to be small ($\alpha < 1$). The unperturbed Hamiltonian

$$\hat{H}^{(0)} = \hat{H}_{\text{el}} + \hat{H}_{\text{ph}} \quad (2.35)$$

has plane waves $|\mathbf{k}\rangle$ as eigenfunctions of the single electron part and many-body basis kets $|n_1 \dots n_q \dots\rangle$ as eigenfunctions of the phonon part. The full eigenkets are given by the composition of the two parts $|\mathbf{k}; \{n_q\}\rangle = |\mathbf{k}\rangle |n_1 \dots n_q \dots\rangle$. The energy of this state is

$$E_{\mathbf{k}, \{n_q\}}^{(0)} = \frac{\hbar^2 \mathbf{k}^2}{2m} + \hbar \omega_{\text{LO}} \sum n_q \quad (2.36)$$

and the ground state is given by an electron with $\mathbf{k} = 0$ and the vacuum state $|0\rangle$ for the phonon part. First-order perturbation theory results in no energy shift, since

$$\langle \mathbf{k} | \langle 0 | (\hat{b}_{\mathbf{q}} + \hat{b}_{-\mathbf{q}}^\dagger) | 0 \rangle | \mathbf{k} \rangle = 0 \quad (2.37)$$

Going to second order

$$\Delta E_{\mathbf{k}}^{(2)} = \sum_{\alpha \neq \{k;0\}} \frac{|\langle \mathbf{k}; 0 | \hat{H}_{\text{el-ph}} | \alpha \rangle|^2}{E_{\{k;0\}} - E_{\alpha}} = \sum_{\alpha \neq \{k;0\}} \frac{\left| \langle \mathbf{k}; 0 | M_{\mathbf{q}} \hat{c}_{\mathbf{k}}^{\dagger} \hat{c}_{\mathbf{k}-\mathbf{q}} (\hat{b}_{\mathbf{q}} + \hat{b}_{-\mathbf{q}}^{\dagger}) | \alpha \rangle \right|^2}{E_{\{k;0\}} - E_{\alpha}} \quad (2.38)$$

where $|\alpha\rangle$ is an excited state. The only states that contribute with non-null terms are states composed of an electron and a single phonon of wavevector \mathbf{q} . The electron is scattered by the phonon in a state of wavevector $\mathbf{k} - \mathbf{q}$, so that the total momentum is conserved. The kets $|\alpha\rangle$ are thus of the form $|\mathbf{k} - \mathbf{q}; n_{\mathbf{q}} = 1\rangle$, with energy

$$E_{\alpha} = \frac{\hbar^2}{2m}(\mathbf{k} - \mathbf{q})^2 + \hbar\omega_{\text{LO}} = \frac{\hbar^2 \mathbf{k}^2}{2m} - \frac{\hbar^2 \mathbf{k} \cdot \mathbf{q}}{m} + \frac{\hbar^2 \mathbf{q}^2}{2m} + \hbar\omega_{\text{LO}} \quad (2.39)$$

The shift in the energy is then

$$\Delta E_{\mathbf{k}} = - \sum_{\mathbf{q}} \frac{|M_{\mathbf{q}}|^2}{\hbar\omega_{\text{LO}} + \frac{\hbar^2}{2m} \mathbf{q}^2 - \frac{\hbar^2}{m} \mathbf{k} \cdot \mathbf{q}} \quad (2.40)$$

We may denote

$$|M_{\mathbf{q}}|^2 = \frac{C}{\mathbf{q}^2} \quad (2.41)$$

where

$$C = (\hbar\omega_{\text{LO}})^2 \left(\frac{\hbar}{2m\omega_{\text{LO}}} \right)^{1/2} \left(\frac{4\pi\alpha}{\Omega} \right) \quad (2.42)$$

Defining $\mu = \frac{\mathbf{k} \cdot \mathbf{q}}{|\mathbf{k}| |\mathbf{q}|}$, we can convert the sum in Eq. (2.40) in an integral,

$$\sum_{\mathbf{q}} \rightarrow \frac{\Omega}{(2\pi)^3} \int d\mathbf{q} = \frac{\Omega}{(2\pi)^3} \int 2\pi q^2 dq d\mu \quad (2.43)$$

then,

$$\Delta E_{\mathbf{k}} = - \frac{\Omega}{(2\pi)^2} \int_{-1}^1 d\mu \int_0^{q_{\text{BZ}}} dq \frac{C}{\hbar\omega_{\text{LO}} + \frac{\hbar^2}{2m} q^2 - \frac{\hbar^2}{m} k q \mu} \quad (2.44)$$

where the integral is extended until the boundary of the first Brillouin zone. Although the integral in Eq. (2.44) may be exactly solved, we can gain some insights on the main physical meaning by developing it in powers of k and letting $q_{\text{BZ}} \rightarrow \infty$. Choosing an appropriate set of units, so that $\hbar = \omega_{\text{LO}} = 2m = 1$,

$$\Delta E_{\mathbf{k}} = - \frac{\alpha}{\pi} \left[2 \int_0^\infty dq \frac{1}{1+q^2} + 4k^2 \int_{-1}^1 d\mu \int_0^\infty dq \frac{q^2 \mu^2}{(1+q^2)^3} \right] = -\alpha - \frac{\alpha}{6} k^2 \quad (2.45)$$

and plugging back the standard units,

$$\Delta E_{\mathbf{k}} = -\alpha \hbar\omega_{\text{LO}} - \frac{\alpha \hbar^2}{6 2m} k^2 \quad (2.46)$$

Finally, the perturbed energy is

$$\epsilon_{\mathbf{k}} = -\alpha\hbar\omega_{\text{LO}} + \left(1 - \frac{\alpha}{6}\right) \frac{\hbar^2}{2m} k^2 \quad (2.47)$$

where the factor on the right can be interpreted as an electron with a new effective mass $m^* = m/(1 - \alpha/6)$. The band energy is shifted down by an overall factor of $\alpha\hbar\omega_{\text{LO}}$ and the effective mass of the electron is increased. This is a reasonable conclusion: the electron digs itself a hole in the lattice potential, lowering its energy, and it has to carry the deformation along its path, resulting in a bigger effective mass.

It is also possible to compute the average number of phonons coupled with the electron at $T = 0$ K. The phonon number operator is given by

$$\hat{N}_{\text{ph}} = \sum_{\mathbf{q}} \hat{b}_{\mathbf{q}}^\dagger \hat{b}_{\mathbf{q}} \quad (2.48)$$

so its average value is

$$\langle \hat{N}_{\text{ph}} \rangle = \sum_{\mathbf{q}} \langle \psi | \hat{b}_{\mathbf{q}}^\dagger \hat{b}_{\mathbf{q}} | \psi \rangle \quad (2.49)$$

where $|\psi\rangle$ is the electron-phonon ket. The ket can be expanded near a state with no phonons $|\mathbf{k}, 0\rangle$

$$|\psi_{\mathbf{k}}\rangle = |\mathbf{k}, 0\rangle + |\delta\psi_{\mathbf{k}}\rangle \quad (2.50)$$

where $|\delta\psi_{\mathbf{k}}\rangle$ is the variation of the wavefunction due to the electron-phonons interaction. Using first-order perturbation theory, it can be found that

$$|\delta\psi_{\mathbf{k}}\rangle = \sum_{a \neq \{\mathbf{k}, 0\}} |a\rangle \frac{\langle \mathbf{k}; 0 | \hat{H}_{\text{el-ph}} | a \rangle}{E_{\{\mathbf{k}, 0\}} - E_a} = \sum_{\mathbf{q}} |\mathbf{k} - \mathbf{q}; n_{\mathbf{q}} = 1\rangle \frac{M_{\mathbf{q}}}{E_{\{\mathbf{k}, 0\}} - E_{\{\mathbf{k} - \mathbf{q}, n_{\mathbf{q}} = 1\}}} \quad (2.51)$$

Inserting the result in Eq. (2.49), we obtain

$$\langle \hat{N}_{\text{ph}} \rangle = \sum_{\mathbf{q}} \frac{\langle \mathbf{k} - \mathbf{q}; n_{\mathbf{q}} = 1 | \hat{b}_{\mathbf{q}}^\dagger \hat{b}_{\mathbf{q}} | \mathbf{k} - \mathbf{q}; n_{\mathbf{q}} = 1 \rangle}{(\hbar\omega_{\text{LO}} + \frac{\hbar^2}{2m} q^2 - \frac{\hbar^2}{m} \mathbf{k} \cdot \mathbf{q})^2} |M_{\mathbf{q}}|^2 \quad (2.52)$$

and substituting q and μ as before,

$$\langle \hat{N}_{\text{ph}} \rangle = \sum_{\mathbf{q}} \frac{|M_{\mathbf{q}}|^2}{(\hbar\omega_{\text{LO}} + \frac{\hbar^2}{2m} q^2 - \frac{\hbar^2}{m} k q \mu)^2} \quad (2.53)$$

or, expressed in our usual set of units,

$$\langle \hat{N}_{\text{ph}} \rangle = \sum_{\mathbf{q}} \frac{|M_{\mathbf{q}}|^2}{(1 + q^2 - \frac{kq}{2} \mu)^2} \quad (2.54)$$

Converting the sum into an integral, inserting Eq. (2.41), and expanding to the lowest order in k , we find

$$\langle \hat{N}_{ph} \rangle = \frac{\Omega}{(2\pi)^2} \frac{4\pi\alpha}{\Omega} \int_0^\infty \frac{4\pi}{(1+q^2)^2} dq = \frac{\alpha}{2} \quad (2.55)$$

The meaning of the parameter α is now more clear: it is a measure of the number of phonons coupled with the electron in the polaron.

2.2.3 Strong coupling limit

In the strong coupling regime, perturbation theory cannot be applied. However, it is possible to use a different approximation method: variational analysis. When the coupling is strong, we expect the electron to dig itself a deeper hole in the lattice potential. The electron will then localize inside the hole. In this regime, we can suppose the polaron wavefunction to be composed of two factors: an unknown phonon wavefunction $|\phi_{ph}\rangle$ and an electron wavefunction $|\psi_{el}\rangle$. The latter is assumed to have the shape of a Gaussian

$$\psi(r) = \frac{1}{r_p^{3/2}} e^{-\frac{r^2}{2r_p^2}} \quad (2.56)$$

where r_p is the effective radius of the polaron, which we use as variational parameter. According to variational theory, we have to minimize the functional

$$\langle \phi_{ph} | \langle \psi_{el} | \hat{H} | \psi_{el} \rangle | \phi_{ph} \rangle \quad (2.57)$$

where \hat{H} is the Fröhlich Hamiltonian

$$\hat{H} = \sum_k \frac{\hbar^2 k^2}{2m} + \sum_q \hbar\omega_{LO} \left(\hat{b}_q^\dagger \hat{b}_q + \frac{1}{2} \right) + \sum_q M_q e^{iq \cdot r} (\hat{b}_q + \hat{b}_{-q}^\dagger) \quad (2.58)$$

and M is the usual interaction matrix derived in Eq. (2.30). In the natural units introduced in the previous section, the Hamiltonian becomes

$$\hat{H} = \sum_k k^2 + \sum_q \left(\hat{b}_q^\dagger \hat{b}_q + \frac{1}{2} \right) + \sum_q M_q e^{iq \cdot r} (\hat{b}_q + \hat{b}_{-q}^\dagger) \quad (2.59)$$

Using the kinetic energy

$$E_{kin} = \langle \psi_{el} | \mathbf{k}^2 | \psi_{el} \rangle = \frac{3}{2r_p^2} \quad (2.60)$$

and the electron density

$$\rho_q = \langle \psi_{el} | e^{iq \cdot r} | \psi_{el} \rangle = e^{-q^2 r_p^2 / 4} \quad (2.61)$$

we find

$$\langle \Psi_{\text{el}} | \hat{H} | \Psi_{\text{el}} \rangle = E_{\text{kin}} + \sum_{\mathbf{q}} \left[\hat{b}_{\mathbf{q}}^\dagger \hat{b}_{\mathbf{q}} + \frac{1}{2} + M_{\mathbf{q}} \rho_{\mathbf{q}} \hat{b}_{\mathbf{q}} + M_{\mathbf{q}}^* \rho_{\mathbf{q}}^* \hat{b}_{\mathbf{q}}^\dagger \right] \quad (2.62)$$

Ignoring the phonon ground state energy and completing the square, we find

$$\langle \Psi_{\text{el}} | \hat{H} | \Psi_{\text{el}} \rangle = E_{\text{kin}} + \sum_{\mathbf{q}} \left(\hat{b}_{\mathbf{q}}^\dagger + M_{\mathbf{q}} \rho_{\mathbf{q}} \right) \left(\hat{b}_{\mathbf{q}} + M_{\mathbf{q}}^* \rho_{\mathbf{q}}^* \right) - \sum_{\mathbf{q}} |M_{\mathbf{q}} \rho_{\mathbf{q}}|^2 \quad (2.63)$$

The second term is easily understandable as a displaced harmonic oscillator. The equilibrium position is shifted from zero by $M_{\mathbf{q}} \rho_{\mathbf{q}}$. This is precisely the effect of the polarization induced by the electron. It is clear that the minimum of the functional will correspond to the vacuum state of the displaced operator. In this state, the energy is simply

$$E_{\text{var}} = \langle \Psi_{\text{el}} | \hat{H} | \Psi_{\text{el}} \rangle = E_{\text{kin}} - \sum_{\mathbf{q}} |M_{\mathbf{q}} \rho_{\mathbf{q}}|^2 \quad (2.64)$$

Converting the sum in an integral, integrating over the angular part, and inserting Eq. (2.41) and Eq. (2.61), the second term becomes

$$\frac{\Omega}{(2\pi)^3} \int_0^\infty 4\pi q^2 \frac{C}{q^2} e^{-q^2 r_p^2/2} dq = \sqrt{\frac{2}{\pi}} \frac{\alpha}{r_p} \quad (2.65)$$

Thus, the variational energy is

$$E_{\text{var}} = \frac{3}{2r_p^2} - \sqrt{\frac{2}{\pi}} \frac{\alpha}{r_p} \quad (2.66)$$

and it is minimized for

$$r_p = \sqrt{\frac{\pi}{2}} \frac{3}{\alpha} \quad (2.67)$$

Plugging back standard units, the final energy is then

$$E_{\text{var}} = -\frac{\alpha^2}{3\pi} \hbar\omega_{\text{LO}} \quad (2.68)$$

If we confront it with the result obtained in Eq. (2.47) using perturbation theory, we see that, for the ground state, the dependence on α is proportional to $-\alpha^2$ instead of $-\alpha$. The variational energy is then lower than the perturbation energy for large α , which is the region of validity of the assumptions we made.

2.3 HOLSTEIN POLARONS

Holstein proposed a different Hamiltonian to model polarons. The main difference is in how the lattice is treated. Instead of working with a continuum, polarizable medium like Fröhlich, Holstein took into account the discreteness of the lattice.

The model is based on the tight-binding model, which was briefly introduced in Section 1.2.3. In the next sections, we will use it to derive Holstein Hamiltonian for a 1D system, and solve it in the weak coupling limit.

2.3.1 Derivation of the Holstein Hamiltonian

We now use the tight-binding model to sketch the derivation of the Holstein Hamiltonian. This Hamiltonian is used to model small polarons, since it treats the polarizable medium as a lattice.

To simplify the derivation, we consider a linear chain of N atoms. At equilibrium, the atom n is placed at the position $R_n = n\alpha$, where α is the lattice constant. The atoms are allowed to move, and their interaction energy is given by the harmonic oscillator approximation. The Hamiltonian of the lattice is then

$$\hat{H}_{I-I} = \sum_n \left(\frac{P_n^2}{2M} + \frac{1}{2} M \omega_0^2 x_n^2 \right) \quad (2.69)$$

where P_n is the momentum of the n^{th} atom, x_n the separation between the atoms n and $n+1$ and M the mass.

The electrons are allowed to interact with the lattice through a potential

$$U = \sum_n U(r - R_n, x_n) \quad (2.70)$$

The key feature of this model is that U depends on the interatomic separation x_n . This results in the coupling of the electrons with the lattice vibrations, so with phonons. Adding the electron kinetic energy term, the total Hamiltonian is given by

$$\hat{H} = \sum_n \left(-\frac{\hbar^2}{2M} \frac{\partial^2}{\partial x_n^2} + \frac{1}{2} M \omega_0^2 x_n^2 \right) - \frac{\hbar^2}{2m} \frac{\partial^2}{\partial r^2} + \sum_n U(r - R_n, x_n) \quad (2.71)$$

Following the tight-binding approach described in Section 1.2.3, we express the electrons wavefunctions as a linear combination of the single atomic orbitals

$$\psi(r) = \sum_n \alpha_n(x_1 \dots x_N) \phi_n(r - n\alpha, x_n) \quad (2.72)$$

where α_n complex coefficients and ϕ_n are the solutions of the corresponding Schrödinger equations

$$\left[-\frac{\hbar^2}{2m} \frac{\partial^2}{\partial r^2} + U(r - n\alpha, x_n) \right] \phi_n = E_n(x_n) \phi_n \quad (2.73)$$

This results in a differential equation for the coefficients α_n , which is obtained through a standard projection procedure. The full calculation can be found in the Appendix of the original Holstein paper [6]. We only report the result

$$\begin{aligned} & \left[i\hbar \frac{\partial}{\partial t} - \sum_p \left(-\frac{\hbar^2}{2M} \frac{\partial^2}{\partial x_p^2} + \frac{1}{2} M \omega_0^2 x_p^2 \right) - E(x_n) - W_n(x_1 \dots x_N) \right] \alpha_n(x_1 \dots x_N) \\ &= \sum_{(\pm)} J(x_n, x_{n+1}) \alpha_{n\pm 1}(x_1 \dots x_N) \end{aligned} \quad (2.74)$$

where

$$W_n(x_1 \dots x_N) = \int |\phi_n(r - na, x_n)|^2 \sum_{p \neq n} U(r - pa, x_p) dr \quad (2.75)$$

$$J(x_n, x_m) = \int \phi_n^*(r - na, x_n) U(r - na, x_n) \phi(r - ma, x_m) dr \quad (2.76)$$

We can simplify Eq. (2.74) introducing three approximations:

1. The neglect of the energies $W_n(x_1 \dots x_N)$.
2. The neglect of the x -dependance of J . The function $J(x_n, x_m)$ reduces to a constant $-J$, which can also be denominated $-t$. It corresponds to the parameter t introduced in the tight-binding approximation in Eq. (1.61).
3. The x -dependance of the energy $E_n(x_n)$ is taken to be linear: $E_n(x_n) = -Ax_n$

The physical meaning of the first approximation (1) is to neglect the perturbation of the wavefunction localized on the site n caused by the interaction with other sites p . This assumption is reasonable in the tight-binding model that we are employing. The result is that the expectation value of the energy of an electron is only dependent on one coordinate x_n , the one of the site where the electron is localized.

With the previous simplifications, Eq. (2.74) becomes

$$i\hbar \frac{\partial}{\partial t} \alpha_n = \sum_p \left(-\frac{\hbar^2}{2M} \frac{\partial^2}{\partial x_p^2} + \frac{1}{2} M\omega_0^2 x_p^2 \right) \alpha_n - t(\alpha_{n+1} + \alpha_{n-1}) \alpha_n - Ax_n \alpha_n \quad (2.77)$$

A study of Eq. (2.77) in its current form is presented by Holstein in his paper [6]. However, we will follow a different approach, expressing it in the second-quantization formalism. From now on, we also consider again a 3D system, generalizing the results that we obtain for the 1D one.

The first term of Eq. (2.77) is exactly the lattice interaction term we have already encountered in Eq. (1.70). In the momentum space, its second-quantized form is given by Eq. (1.72)

$$\hat{H}_{ph} = \hbar\omega_0 \sum_q \left(\hat{b}_q^\dagger \hat{b}_q + \frac{1}{2} \right) \quad (2.78)$$

where we have assumed the phonons to be dispersionless and optical, as we did for the Fröhlich Hamiltonian. The second term is the tight-binding energy encountered in Section 1.2.3 and its second-quantized form is give by Eq. (1.64)

$$\hat{H}_{el} = \sum_k \epsilon_k^{tb} \hat{c}_k^\dagger \hat{c}_k \quad (2.79)$$

Finally, the last term is responsible for the electron-phonon interaction energy. We have seen that, for a normal scattering process, the general form of the interaction matrix is

given by Eq. (1.96). Since in this case the interaction amplitude is independent of the momentum, we can write the interaction matrix as constant g in the position space and g/\sqrt{N} in the momentum space. The interaction Hamiltonian is then given by Eq. (1.86)

$$\hat{H}_{\text{el-ph}} = \frac{g}{\sqrt{N}} \sum_{\mathbf{k}, \mathbf{q}} \hat{c}_{\mathbf{k}+\mathbf{q}}^\dagger \hat{c}_{\mathbf{k}} (\hat{b}_{-\mathbf{q}}^\dagger + \hat{b}_{\mathbf{q}}) \quad (2.80)$$

The final Holstein Hamiltonian is

$$\hat{H}_{\text{Holstein}} = \sum_{\mathbf{k}} \epsilon_{\mathbf{k}}^{\text{tb}} \hat{c}_{\mathbf{k}}^\dagger \hat{c}_{\mathbf{k}} + \hbar\omega_0 \sum_{\mathbf{q}} \left(\hat{b}_{\mathbf{q}}^\dagger \hat{b}_{\mathbf{q}} + \frac{1}{2} \right) + \frac{g}{\sqrt{N}} \sum_{\mathbf{k}, \mathbf{q}} \hat{c}_{\mathbf{k}+\mathbf{q}}^\dagger \hat{c}_{\mathbf{k}} (\hat{b}_{-\mathbf{q}}^\dagger + \hat{b}_{\mathbf{q}}) \quad (2.81)$$

2.3.2 Weak coupling limit

Like the Fröhlich Hamiltonian, the Holstein Hamiltonian is not exactly solvable in its general form. Although it is exactly solvable for a two state system [22], we will use perturbation theory to find an approximated solution. We will follow the same procedure we adopted in Section 2.2.2. This method is valid as long as the coupling constant

$$\alpha = \frac{g^2}{z\hbar\omega_0 t} \quad (2.82)$$

where z is the dimensionality of the problem, is small.

We start by splitting the Holstein Hamiltonian in an unperturbed term $\hat{H}^{(0)} = \hat{H}_{\text{el}} + \hat{H}_{\text{ph}}$ and the perturbation $\hat{H}_{\text{el-ph}}$. The solution to the unperturbed problem is found solving the Hamiltonian

$$\hat{H}^{(0)} = \sum_{\mathbf{k}} \epsilon_{\mathbf{k}}^{\text{tb}} \hat{c}_{\mathbf{k}}^\dagger \hat{c}_{\mathbf{k}} + \hbar\omega_0 \sum_{\mathbf{q}} \left(\hat{b}_{\mathbf{q}}^\dagger \hat{b}_{\mathbf{q}} \right) \quad (2.83)$$

where we have ignored the ground-state phonon energy and where

$$\epsilon_{\mathbf{k}}^{\text{tb}} = -t \sum_{\delta} \cos(\mathbf{k} \cdot \mathbf{R}_{\delta}) \quad (2.84)$$

where δ is an index of the nearest neighbours. Working in one dimension, considering a linear chain of atoms separated by a unitary distance, Eq. (2.84) becomes

$$\epsilon_{\mathbf{k}}^{\text{tb}} = -2t \cos(k) \quad (2.85)$$

where the factor two arises from the fact that there are two nearest neighbours for each ion.

If we separate the polaron ket in its electron and phonon part $|\mathbf{k}, \mathbf{n}_q\rangle = |\mathbf{k}\rangle |n_1 \dots n_q \dots\rangle$ we can find its unperturbed energy

$$E_{\mathbf{k}, \mathbf{n}_q}^{(0)} = -t \sum_{\delta} \cos(k) + \hbar\omega_0 \sum_{\mathbf{q}} n_{\mathbf{q}} \quad (2.86)$$

We are now ready to add the perturbation

$$\hat{H}_{\text{el-ph}} = \frac{g}{\sqrt{N}} \sum_{k,q} \hat{c}_{k+q}^\dagger \hat{c}_k (\hat{b}_{-q}^\dagger + \hat{b}_q) \quad (2.87)$$

The form of this Hamiltonian is totally analogous to the Fröhlich Hamiltonian we have encountered in Section 2.2.2, with $\frac{g}{\sqrt{N}}$ in place of M_q . With analogous considerations, we can than conclude that the only states that give rise to non-null terms in the second-order energy correction

$$\Delta E_k^{(2)} = \sum_{a \neq \{k,0\}} \frac{|\langle k;0 | \hat{H}_{\text{el-ph}} | a \rangle|^2}{E_{\{k,0\}} - E_a} = \frac{g^2}{N} \sum_{a \neq \{k,0\}} \frac{|\langle k;0 | \hat{c}_k^\dagger \hat{c}_{k-q} (\hat{b}_q + \hat{b}_{-q}^\dagger) | a \rangle|^2}{E_{\{k,0\}} - E_a} \quad (2.88)$$

are states with an electron of momentum $k - q$ and a single phonon of momentum q . Using Eq. (2.85) we can find the energy of the ground state

$$E_{k,0}^{(0)} = -2t \cos(k) \quad (2.89)$$

and of the excited state

$$E_a = E_{k,n_q=1}^{(0)} = -2t \cos(k - q) + \hbar\omega_0 \quad (2.90)$$

Plugging Eqs. (2.89) and (2.90) in Eq. (2.88) and replacing the sum with an integral as we did in Section 2.2.2, we find

$$\begin{aligned} \Delta E_k &= -\frac{1}{2\pi} \int dq \frac{g^2}{2t \cos(k) + 2t \cos(k - q) - \hbar\omega_0} \\ &= -\frac{1}{2\pi} \int dq \frac{\alpha \hbar\omega_0 t}{2t \cos(k) + 2t \cos(k - q) - \hbar\omega_0} \end{aligned} \quad (2.91)$$

The total energy is then

$$E_k = -2t \cos(k) - \frac{1}{2\pi} \int dq \frac{\alpha \hbar\omega_0 t}{2t \cos(k) + 2t \cos(k - q) - \hbar\omega_0} \quad (2.92)$$

2.4 SMALL AND LARGE POLARONS

In the previous sections, we have divided polarons in two categories: small and large. A small polaron is defined as a polaron that is created by a distortion of the lattice smaller than the unit cell. Conversely, a large polaron originates from a distortion bigger than the unit cell. The distinction can also be made in terms of the strength of the electron-phonon coupling. When it is strong, electrons are localized around a single atom and only the interactions with the nearest-neighbours atoms are relevant. When

the interaction is weak, longer-range interactions becomes more significant. A picture of the charge isosurfaces of a small and large polaron is given in Fig. 1

We have seen how the two types of polarons are usually described with two different Hamiltonians. The Fröhlich Hamiltonian is typically used for large polarons, where the discreteness of the lattice plays a minor role. For this reason, large polarons are often also called Fröhlich polarons. On the other hand, small polarons - which are also called Holstein polarons - are described by the Holstein Hamiltonian, which takes into account the discrete behaviour of the lattice more accurately.

The differences between small and large polarons are more than just their sizes. A very important one is their mobility [23]. Polarons form in polarizable materials, such ionic crystals or polar semiconductors. In both cases, electronic transport occur via hopping. The charges are thermally activated over a gap, and hop from one site to another. However, if in semiconductors the charges must have enough energy to jump over the band gap, in polaronic materials the gap is much narrower. In fact, polarons have to jump from a localized state (the polaronic band) to the conduction band.

Several different diffusion mechanisms have been identified to describe polarons mobility. However, a simplified picture can be drawn to highlight the general differences between small and large polarons [24]. Small polarons typically hop from one site to another assisted by phonons, when the distortion of the polaron's site is disturbed by thermal vibrations. The resulting motion is thus incoherent, and the mobility is usually much smaller than $1 \text{ cm}^2 \text{V}^{-1} \text{s}^{-1}$. The mobility increases with temperature, since this increases the thermal vibrations which cause the hoping. Conversely, large polarons tend to follow a quasi-free-carrier-like motion. We have seen that the effective mass is greater for polarons than for free-charge. Since the large effective mass prevents them from scattering with the phonon field, this results in a higher mobility. The mobility is reduced by the increasing of temperature, which makes the scattering more effective.

The property of small and large polarons discussed above are summarized in Table 1.

Table 1: Summary of small and large polarons properties. The table is taken from Franchini's review on polarons [24]

Small (Holstein) polarons	Large (Fröhlich) polarons
$\hat{H}_{\text{el-ph}} = \frac{g}{\sqrt{N}} \sum_{\mathbf{k}, \mathbf{q}} \hat{c}_{\mathbf{k}+\mathbf{q}}^\dagger \hat{c}_{\mathbf{k}} (\hat{b}_{-\mathbf{q}}^\dagger + \hat{b}_{\mathbf{q}})$	$\hat{H}_{\text{el-ph}} = \sum_{\mathbf{k} \mathbf{q}} M_{\mathbf{q}} \hat{c}_{\mathbf{k}}^\dagger \hat{c}_{\mathbf{k}-\mathbf{q}} (\hat{b}_{\mathbf{q}} + \hat{b}_{-\mathbf{q}}^\dagger)$
<ul style="list-style-type: none"> • Short-range electron-phonon interaction • Polaron radius \approx lattice parameter • Narrow mid-gap electronic state (≈ 1 eV below E_F) • Incoherent motion (phonon assisted) • Thermally activated hopping mobility $\ll 1 \text{ cm}^2 \text{V}^{-1} \text{s}^{-1}$ • Mobility increasing with temperature 	<ul style="list-style-type: none"> • Long-range electron-phonon interaction • Polaron radius \gg lattice parameter • Shallow mid-gap electronic state (≈ 10 eV below E_F) • Coherent motion • Free carrier mobility $\gg 1 \text{ cm}^2 \text{V}^{-1} \text{s}^{-1}$ • Mobility decreasing with temperature

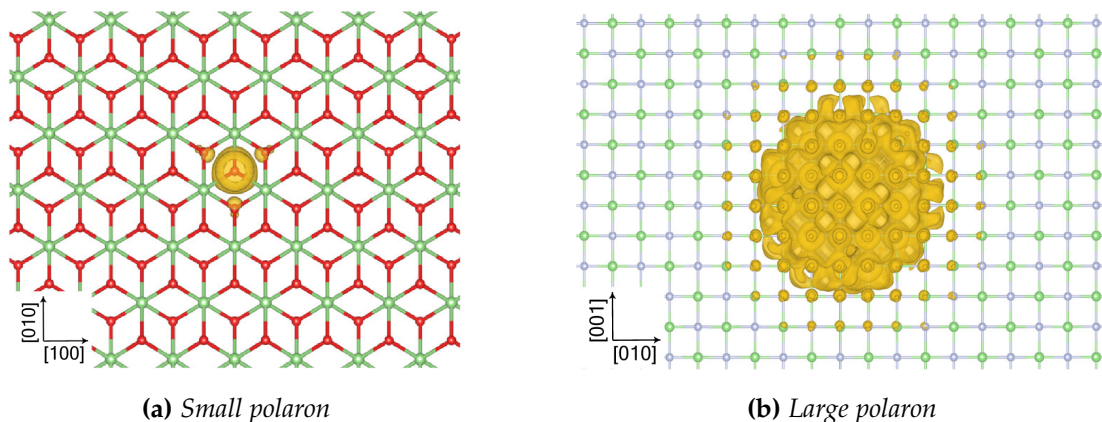


Figure 1: Example of charge isosurfaces of a small and a large polaron in a 2D lattice. The images are taken from Sio et al. [11]

3

DENSITY FUNCTIONAL THEORY

Condensed Matter Physics often has to deal with systems of many interacting particles, typically electrons. We have already introduced a mathematical formalism that allows to describe such systems. However, the resulting Hamiltonians often do not have analytical solutions. In these cases, we rely on numerical simulations. One particular approach has emerged as a popular choice in the last decades: Density Functional Theory (DFT). It is based on two seminal papers, respectively written by Hohenberg and Kohn [25] and Kohn and Sham [26]. DFT allows us to solve many-electrons problems in an *ab-initio* fashion. It is effective for understanding properties related to the electronic ground state of a system. The key advantage of this formalism is that it provides a means to transform a many interacting electrons problem to an effective-field one-electron self-consistent problem, which is exact in principle.

In the next sections we will introduce this formalism and its application, focusing on VASP (Vienna Ab-initio Simulation Package).

3.1 INTRODUCTION TO DFT

3.1.1 *Ground state and density functional formalism*

The basic assumption of DFT is that, for a system of interacting electrons in an external potential $v(\mathbf{r})$, the ground-state energy E_g can be expressed as a functional of the sole charge density $\rho(\mathbf{r})$. We will indicate this with the standard notation $E_g[\rho]$. This statement was proven for the first time by Hohenberg and Kohn in 1964 [25]. This allows a great simplification of the original problem, since the ground-state energy depends only on a single scalar field $\rho(\mathbf{r})$, instead on a multi-particle wavefunction $\Psi(\mathbf{r}_1 \dots \mathbf{r}_N)$. The external potential is usually assumed to be the ionic potential.

We want to show that we can write E_g as a functional of $\rho(\mathbf{r})$ only. We will take the point of view that our problem is entirely determined by the external potential $v(\mathbf{r})$. In fact, the Hamiltonian can be expressed as a sum of three components

$$\hat{H} = \sum_i v(\mathbf{r}_i) + \sum_i \frac{\mathbf{p}_i^2}{2m} + \frac{1}{2} \sum_{i \neq j} \frac{e^2}{|\mathbf{r}_i - \mathbf{r}_j|} = V + T + U \quad (3.1)$$

If we have a system of N electrons and we want to determine its ground-state energy, the last two terms (T and U) are universal for all such problems. The solution Ψ is then entirely determined by the first term V . If we define

$$\rho(\mathbf{r}) = \sum_i \langle \Psi | \delta^3(\mathbf{r} - \mathbf{r}_i) | \Psi \rangle \quad (3.2)$$

since Ψ is determined by V , ρ is a unique functional of V . The main point of the theory is that also the converse is true. We can prove it by contradiction.

Let's assume that the contrary is true. That is, there exists another external potential $v'(\mathbf{r})$ such that the ground state solution of the respective Schrödinger equation $|\Psi'\rangle$ gives the same density $\rho'(\mathbf{r}) = \rho(\mathbf{r})$. The two potentials are assumed to differ for more than a constant. Since $|\Psi'\rangle$ and $|\Psi\rangle$ are solutions to Schrödinger equations with different potentials, they will differ for more than a phase factor. We know from variational theory that the ground-state wavefunction minimizes the expectation value of the Hamiltonian, so

$$E' = \langle \Psi' | H' | \Psi' \rangle < \langle \Psi | H' | \Psi \rangle \quad (3.3)$$

but

$$\langle \Psi | H' | \Psi \rangle = \langle \Psi | H - V + V' | \Psi \rangle = E + \int [v'(\mathbf{r}) - v(\mathbf{r})] \rho(\mathbf{r}) d\mathbf{r} \quad (3.4)$$

which leads to the inequality

$$E' < E + \int [v'(\mathbf{r}) - v(\mathbf{r})] \rho(\mathbf{r}) d\mathbf{r} \quad (3.5)$$

Similarly, for the primed system, we find

$$E < E' + \int [v(\mathbf{r}) - v'(\mathbf{r})] \rho'(\mathbf{r}) d\mathbf{r} \quad (3.6)$$

Adding the previous two equations, remembering that $\rho'(\mathbf{r}) = \rho(\mathbf{r})$, we get

$$E' + E < E + E' \quad (3.7)$$

which is obviously absurd. This proves that $v(\mathbf{r})$ is a unique functional of $\rho(\mathbf{r})$. In other words, given a physical electron density, there is a unique external potential that may cause it. In addition, since knowing $v(\mathbf{r})$ defines completely the problem, $|\Psi\rangle$ is also a functional of $\rho(\mathbf{r})$.

We can define a new functional

$$F[\rho] = \langle \Psi[\rho] | T + U | \Psi[\rho] \rangle \quad (3.8)$$

and, using Eq. (3.1), express the ground-state energy as

$$E_g[\rho] = \langle \Psi[\rho] | V + T + U | \Psi[\rho] \rangle = \int v(\mathbf{r}) \rho(\mathbf{r}) d\mathbf{r} + F[\rho] \quad (3.9)$$

where $v(\mathbf{r})$ is a functional of ρ . The problem is than now reduced to minimizing the functional $E_g[\rho]$ with the constraint $N = \int \rho(\mathbf{r})d\mathbf{r}$. If $F[\rho]$ had a simple known expression, the problem would be quite straight forward. Unfortunately, this in not the case, and the expression of $F[\rho]$ is not explicitly known.

3.1.2 The Kohn-Sham Equations

Kohn and Sham proved in 1965 that $\rho(\mathbf{r})$ can be determined solving a set of N Shrödinger-type equations, subject to an effective potential $v'(\mathbf{r})$. It is important to emphasize that the solutions of the N equations should not be interpreted as orbitals of the real system. In the Kohn-Sham formalism two different systems are considered: the real system, made of N interacting particles subject to an external potential $v(\mathbf{r})$, and a fictitious system, made of N non-interacting particles subject to an effective potential $v'(\mathbf{r})$.

In the expression of the ground-state energy shown in Eq. (3.9), $F[\rho]$ contains both the kinetic energy T and the interaction energy U , for which there are no known expressions in terms of the density $\rho(\mathbf{r})$. However, we can estimate $F[\rho]$ in some limiting cases. If we neglect exchange and correlation effects, the interaction energy is given by the Hartree term

$$U_{KS} = \frac{e^2}{2} \int \frac{\rho(\mathbf{r})\rho(\mathbf{r}')}{|\mathbf{r} - \mathbf{r}'|} d\mathbf{r} d\mathbf{r}' \quad (3.10)$$

For a non-interacting system of N particles of density $\rho(\mathbf{r})$, where each particle is described by a wavefunction $\phi_i(\mathbf{r})$, the total kinetic energy is given by

$$T_{KS} = -\frac{\hbar^2}{2m} \sum_i \int \phi_i^*(\mathbf{r}) \nabla^2 \phi_i(\mathbf{r}) d\mathbf{r} \quad (3.11)$$

with

$$\rho(\mathbf{r}) = \sum_i \phi_i^*(\mathbf{r}) \phi_i(\mathbf{r}) \quad (3.12)$$

It is reasonable to expect that the interaction and kinetic energy of the real system will be close to the sum of Eq. (3.10) and Eq. (3.11). It is then convenient to write the functional $F[\rho]$ as

$$F[\rho] = T_{KS}[\rho] + U_{KS}[\rho] + E_{xc}[\rho] \quad (3.13)$$

where E_{xc} is added to take into account exchange and correlation effects. Our entire ignorance on $F[\rho]$ is now contained in $E_{xc}[\rho]$. We can express the ground-state energy functional as

$$E_g[\rho] = \int v(\mathbf{r})\rho(\mathbf{r})d\mathbf{r} + T_{KS} + \frac{e^2}{2} \int \frac{\rho(\mathbf{r})\rho(\mathbf{r}')}{|\mathbf{r} - \mathbf{r}'|} d\mathbf{r} d\mathbf{r}' + E_{xc}[\rho] \quad (3.14)$$

It is now time to bring in the fictitious systems we introduced above. Our goal is to determine a second system of N interacting particles with the same density $\rho(\mathbf{r})$

of the real system. The Schrödinger equation of the fictitious system are solved to determine $\rho(\mathbf{r})$. Then, the density is plugged in Eq. (3.14) to determine the value of the ground-state energy functional. Using the variational principles, the non-interacting system is varied to minimize the real system ground state energy. The minimum will give us the charge density and the ground-state energy of the real system. The variation gives rise to a set of Euler-Lagrange equations that governs the single-particle orbitals and energies of the fictitious system.

Let's then consider a non-interacting system of N particles subject to an effective potential $v'(\mathbf{r})$. The density $\rho'(\mathbf{r})$ is determined solving

$$\left(-\frac{\hbar^2}{2m}\nabla^2 + v'(\mathbf{r})\right)\phi_i(\mathbf{r}) = \epsilon_i\phi_i(\mathbf{r}) \quad (3.15)$$

and computing $\rho'(\mathbf{r}) = \sum_i |\phi_i(\mathbf{r})|^2$. The kinetic energy is then given by

$$T_{KS}[\rho'] = \sum_i \epsilon_i - \int v'(\mathbf{r})\rho'(\mathbf{r})d\mathbf{r} \quad (3.16)$$

Inserting this result in Eq. (3.14), we find an expression for the ground-state energy functional

$$\begin{aligned} E_g[\rho'] &= \int v(\mathbf{r})\rho'(\mathbf{r})d\mathbf{r} \\ &\quad + \left(\sum_i \epsilon_i - \int v'(\mathbf{r})\rho'(\mathbf{r})d\mathbf{r} \right) + \frac{e^2}{2} \int \frac{\rho'(\mathbf{r})\rho'(\mathbf{r}')}{|\mathbf{r}-\mathbf{r}'|} d\mathbf{r}d\mathbf{r}' + E_{xc}[\rho'] \end{aligned} \quad (3.17)$$

To obtain the physical density and the actual ground-state energy, we minimize Eq. (3.17) by varying ρ . That is, we evaluate the shift in energy $E_g \rightarrow E_g + \delta E_g$ after a variation $\rho' \rightarrow \rho' + \delta\rho'$

$$\begin{aligned} \delta E_g &= \int v(\mathbf{r})\delta\rho'(\mathbf{r})d\mathbf{r} + \sum_i \delta\epsilon_i - \int \delta\rho'(\mathbf{r}) \left[v'(\mathbf{r}) + \int \frac{\delta v'(\mathbf{r}')}{\delta\rho'(\mathbf{r})} \rho'(\mathbf{r}')d\mathbf{r}' \right] d\mathbf{r} \\ &\quad + e^2 \int \delta\rho'(\mathbf{r}) \frac{\rho'(\mathbf{r}')}{|\mathbf{r}-\mathbf{r}'|} d\mathbf{r}d\mathbf{r}' + \int \delta\rho'(\mathbf{r}) \frac{\delta E_{xc}}{\delta\rho'(\mathbf{r})} d\mathbf{r} \\ &= \sum_i \delta\epsilon_i + \int \delta\rho'(\mathbf{r}) \left[v(\mathbf{r}) - v'(\mathbf{r}) - \int \frac{\delta v'(\mathbf{r}')}{\delta\rho'(\mathbf{r})} \rho'(\mathbf{r}')d\mathbf{r}' + e^2 \int \frac{\rho'(\mathbf{r}')}{|\mathbf{r}-\mathbf{r}'|} d\mathbf{r}' + \frac{\delta E_{xc}}{\delta\rho'(\mathbf{r})} \right] d\mathbf{r} \end{aligned} \quad (3.18)$$

When $\rho'(\mathbf{r})$ minimizes the functional, the previous expression is equal to zero. Minimizing with respect to $\rho'(\mathbf{r})$ is equivalent to doing it with respect to $v'(\mathbf{r})$. Since, to first order in $\delta v'$,

$$\sum_i \delta\epsilon_i = \sum_i \langle \phi_i | \delta v' | \phi_i \rangle = \int \delta v'(\mathbf{r}') \rho'(\mathbf{r}') d\mathbf{r}' = \int \delta\rho'(\mathbf{r}) \frac{\delta v'(\mathbf{r}')}{\delta\rho'(\mathbf{r})} \rho'(\mathbf{r}') d\mathbf{r}d\mathbf{r}' \quad (3.19)$$

setting Eq. (3.18) equals to zero gives

$$v'(\mathbf{r}) = v(\mathbf{r}) + e^2 \int \frac{\rho'(\mathbf{r}')}{|\mathbf{r} - \mathbf{r}'|} d\mathbf{r}' + \frac{\delta E_{xc}}{\delta \rho'(\mathbf{r})} \quad (3.20)$$

The equations that govern the fictitious non-interacting system are then

$$\left(-\frac{\hbar^2}{2m} \nabla^2 + v(\mathbf{r}) + v_H(\mathbf{r}) + v_{xc}(\mathbf{r}) \right) \phi_i(\mathbf{r}) = \epsilon_i \phi_i(\mathbf{r}) \quad (3.21)$$

where

$$v_H(\mathbf{r}) = e^2 \int \frac{\rho'(\mathbf{r}')}{|\mathbf{r} - \mathbf{r}'|} d\mathbf{r}' \quad (3.22)$$

$$v_{xc}(\mathbf{r}) = \frac{\delta E_{xc}}{\delta \rho'(\mathbf{r})} \quad (3.23)$$

and $\rho'(\mathbf{r})$ is given by

$$\rho'(\mathbf{r}) = \sum_i |\phi_i(\mathbf{r})|^2 \quad (3.24)$$

Equations 3.21 are known as Kohn-Sham equations. They look like a set of Schrödinger equations, but they are inherently different. In fact, the LHS of the equations depends on ρ , and so on ϕ_i , like the RHS.

If E_{xc} were exactly known, the equations would be solvable with a self-consistent calculation. In a self-consistent calculation, an initial $\rho(\mathbf{r})$ is assumed and the LHS of the equation is evaluated. Then, the equation is solved like a standard Schrödinger equation, and a new $\rho(\mathbf{r})$ is computed through Eq. (3.24). The solution is plugged in Eq. (3.17) to find the ground-state energy of the real system. The procedure is repeated with the new density, and it ends when the difference in energy between two successive steps is smaller than a pre-chosen value. It is important to emphasize that the coefficients ϵ_i have nothing to do with the energies of the electrons of the interacting system. The only quantities with physical meaning are the total electron density $\rho(\mathbf{r})$ and the ground-state energy E_g .

Since E_{xc} is not exactly known, different approximations have been developed. The different models are developed based on some constraints that the exchange-correlation functional must satisfy. The models are tested on simple systems that are exactly solvable, like the uniform electron gas. The functional are generally parametrized, and the parameters can be set based on *ab-initio* calculations or fitting experimental data.

A common approach is to write E_{xc} as

$$E_{xc} = \int \rho(\mathbf{r}) \epsilon_{xc}(\mathbf{r}) d\mathbf{r} \quad (3.25)$$

The functionals E_{xc} are generally divided in two classes: the local density approximation (LDA) and generalized gradient approximation (GGA). In the LDA, $\epsilon_{xc}(\mathbf{r})$ is assumed

to be dependent on the density $\rho(\mathbf{r})$ only, whereas in the GGA also on its gradient $\nabla\rho(\mathbf{r})$. The functionals take the form

$$E_{xc}^{\text{LDA}} = \int \rho(\mathbf{r}) \epsilon_{xc}(\rho) d\mathbf{r} \quad (3.26)$$

$$E_{xc}^{\text{GGA}} = \int \rho(\mathbf{r}) \epsilon_{xc}(\rho, \nabla\rho) d\mathbf{r} \quad (3.27)$$

3.1.3 DFT corrections: DFT+U

DFT has a good accuracy when determining structural and cohesive properties, but it often fails in the prediction of electronic properties. The fundamental problem of DFT resides in the Hartree term

$$\frac{e^2}{2} \int \frac{\rho'(\mathbf{r})\rho'(\mathbf{r}')}{|\mathbf{r} - \mathbf{r}'|} \quad (3.28)$$

In fact, this term does not exclude the contribution of self-interaction to the electronic repulsion energy. This effect cannot be counterbalanced by the exchange-correlation term, because the form of the two is inherently different. The Hartree term is given by a double integral, whereas the exchange-correlation energy by a single integral.

The effect is that DFT favours delocalized states, which have a lower self-interaction energy. As a result, band gaps energies of semiconductors are usually underestimated [27]. Many alternative solutions have been proposed, like the hybrid functionals and the post-Hartree-Fock methods [28]. However, we will focus on the approach proposed by Anisimov, called DFT+U [29]. This approach has the advantage to be as reliable as the other methods, but with significantly lower computational cost.

The developing of DFT+U was inspired by another model: the Hubbard model. This model is useful to describe the transition between conducting and isolating systems. It is based on the tight-binding approximation: the electrons are described by the usual atomic orbitals and are allowed to "jump" from one atom to the other. The probability of the jump is described by a transfer integral t . The Hubbard model adds to the tight-binding model an on-site repulsion, consequence of the repulsion of the electrons residing in the same orbital. In its simpler formulation, the Hubbard model can be applied to a linear chain of hydrogen atoms. The electrons occupy s orbitals and may have spin up or down. This system can be described by the following Hubbard Hamiltonian

$$\hat{H}_{\text{Hub}} = -t \sum_{\langle i,j \rangle} \hat{c}_{j,\sigma}^\dagger \hat{c}_{j,\sigma} + U \sum_i \hat{n}_{i\uparrow} \hat{n}_{i\downarrow} \quad (3.29)$$

where $\langle i, j \rangle$ indicates two nearest-neighbours atoms, σ is the spin, \hat{c}^\dagger and \hat{c} the creation and annihilation operators and \hat{n} the number operator. The first term is parametrized by the transfer integral t , which represents the kinetic energy of the electron that jumps between the atoms. The second term takes into account the potential energy given by

the repulsion of the electrons. The first term favours delocalized states, whereas the second one tends to localize the electrons.

The original DFT Hamiltonian is corrected adding the Hubbard contribution. This is not done for all the electrons, but only for the electrons that reside in the most localized orbitals (d and f). Electrons in s and p orbitals are treated with standard DFT. The parameters t and U are usually determined semi-empirically, fitting the data from the experimental band gaps. This method was simplified by Dudarev et al. in 1998 [30]. In their model, the intra-atomic self-interaction error is corrected via a Hubbard-like model which depends only on the difference $U - t$. The final effect of using a DFT+U approach instead of doing a standard DFT calculation is the broadening of the band gap. The greater the value assigned to U is, the more the states are localized and the more the gap broadens.

3.2 IMPLEMENTATION

We are now interested in how the theory that we have presented is implemented in simulation programs. DFT is widely used for simulating many systems, from atoms to crystals. However, it is mainly employed to study solid state systems. The main reason is that in crystals, we can take advantage of the symmetries of the system to simplify the computation. We have shown in Section 1.2.1 that crystals are periodic systems, where the periodicity is governed by the lattice vectors \mathbf{R}_n . Every property, included the ion potential, shares the same periodicity. The central consequence is that the solutions to the Schrödinger equation for this kind of potential can be written in a Bloch form

$$\Psi_{\mathbf{k}}(\mathbf{r}) = u_{\mathbf{k}}(\mathbf{r})e^{i\mathbf{k}\cdot\mathbf{r}} \quad (3.30)$$

where \mathbf{k} is the wavevector and $u_{\mathbf{k}}(\mathbf{r})$ is a function with the same periodicity of the lattice, that is $u_{\mathbf{k}}(\mathbf{r}) = u_{\mathbf{k}}(\mathbf{r} + \mathbf{R}_n)$. We can use this fact to expand $u_{\mathbf{k}}(\mathbf{r})$ in a Fourier series

$$u_{\mathbf{k}}(\mathbf{r}) = \sum_{\mathbf{G}} c_{\mathbf{k}+\mathbf{G}} e^{i\mathbf{G}\cdot\mathbf{r}} \quad (3.31)$$

where \mathbf{G} are reciprocal lattice vectors and $c_{\mathbf{k}+\mathbf{G}}$ are constants. The general solution of the Schrödinger equation is then

$$\Psi_{\mathbf{k}}(\mathbf{r}) = \sum_{\mathbf{G}} c_{\mathbf{k}+\mathbf{G}} e^{i(\mathbf{k}+\mathbf{G})\cdot\mathbf{r}} \quad (3.32)$$

Wavefunctions in the Bloch form are not only easier to manage, but they offer significant advantages in performing computations. In fact, solving Eq. (3.21) requires solving many integrals of the form $\langle \Psi_{\mathbf{k}}(\mathbf{r}) | \hat{H} | \Psi_{\mathbf{k}}(\mathbf{r}) \rangle$. For a given value of \mathbf{k} , the integrals should be performed over the whole space. This would be very computationally

demanding. Fortunately, if $\Psi_{\mathbf{k}}(\mathbf{r})$ is a Bloch function, it can be proven that the solution of the integral are given by the sum of the band energies ϵ_n , so

$$\langle \Psi_{\mathbf{k}}(\mathbf{r}) | \hat{H} | \Psi_{\mathbf{k}}(\mathbf{r}) \rangle = \frac{\Omega}{(2\pi)^3} \sum_n \int_{BZ} \epsilon_n(\mathbf{k}) d\mathbf{k} \quad (3.33)$$

where Ω is the volume of the unit cell and the integral is extended over the first Brillouin zone. This integral is much easier to compute. In practical calculations, the integral over the Brillouin zone is evaluated only on a finite set of points. The most common choice for this set of points is the Monkhorst-Pack grid [31]. In fractional coordinates, it is a rectangular grid spaced evenly throughout the Brillouin zone. The main advantage of this method is that it gives accurate results even with a small number of points.

Sometimes, the integration has problems to converge because of the discontinuity points of the function. This is particularly common in metals, where it is common to have regions in the reciprocal space where the electronic density suddenly drops to zero. To avoid this inconvenience, the discontinuity regions are softened applying *smearing* functions. For example, it is common to use Gaussian functions centred in the discontinuity and parametrized by their standard deviation σ . In the limit $\sigma \rightarrow 0$ there is no smearing, and the discontinuity is not eliminated.

The problem of solving the Kohn-Sham equations is not completely solved yet. In fact, in Eq. (3.32) the sum is extended over an infinite number of reciprocal lattice vectors \mathbf{G} , so it is not possible to evaluate it exactly. Luckily, the single terms in the sum may be interpreted as solutions to Schrödinger equations with a corresponding kinetic energy

$$E_{\mathbf{k}} = \frac{\hbar^2(\mathbf{k} + \mathbf{G})^2}{2m} \quad (3.34)$$

The higher energy terms will have less physical meaning, so they can be excluded from the sum. This is done by choosing a cut-off value E_{cut} and a corresponding value \mathbf{G}_{cut} , and ignoring the terms with $|\mathbf{G}| < \mathbf{G}_{\text{cut}}$.

Usually, in DFT applications, another simplification is made. Since most of the properties of materials are determined only by the valence electrons, the ion-electron interaction is determined using pseudopotentials. With pseudopotentials, the core electrons are removed from the calculation, and they are replaced with an effective potential. Only the valence electrons (or the valence and outer core electrons) are simulated. In addition to reducing the number of electrons that have to be simulated, pseudopotentials offer a second advantage. The valence electrons wavefunctions oscillate rapidly near the nucleus because of the strong nuclear potential, as it can be seen in Fig. 2. The rapid oscillations in the region close to the nucleus require high frequency cut-off energies for the plane waves, impacting on the simulation performance. Pseudopotentials "smoothen" the wavefunctions, allowing to choose a smaller \mathbf{G}_{cut} and making the computation faster.

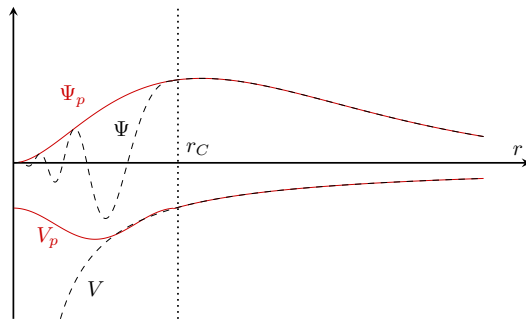


Figure 2: Comparison of a wavefunction in the Coulomb potential of the nucleus (black line) and in a pseudopotential (red line). The wavefunctions and potentials coincide for distances greater than r_C .

3.3 VIENNA AB-INITIO SIMULATION PACKAGE

VASP (Vienna Ab-initio Simulation Package) is a computer program developed by the University of Vienna for DFT calculations [32–35]. This software has been used for all the simulations performed in this thesis. In this section, we will describe how a general simulation in VASP is performed.

The basic elements that VASP needs to perform the simulation are the positions of the atoms in the crystal, the k-space mesh grid used for the computation and the pseudopotentials. Each of this element is given in input to the program through three different files. The first file is named POSCAR, and it contains a description of the crystal. An example is given below

```

1 Cubic diamond          # first line used as comment
2      5.5               # lattice constant (in angstrom)
3 #--- Definition of the basis vectors of the primitive cell---
4   0.0    0.5    0.5    # a1
5   0.5    0.0    0.5    # a2
6   0.5    0.5    0.0    # a3
7 Si                      # atomic species
8 2                       # number of atoms in the primitive cell
9 #--- Positions of the atoms in the primitive cell---
10 Direct                 # Direct: lattice vectors basis
11                         # Cartesian: cartesian basis
12   0.00  0.00  0.00     # first atom
13   0.25  0.25  0.25     # second atom
14                         # [...]

```

The first half of the file describes the lattice. The lattice is defined through the three basis vectors \mathbf{a}_1 , \mathbf{a}_2 and \mathbf{a}_3 . These vectors are given by multiplying the lattice constants defined in line 2 with the vectors defined in lines 4-6. The second half of the file describes the composition of the primitive cell. Lines 7 and 8 define the type and

number of atoms in the cell, whereas line 12-13 their positions. The positions can be expressed in cartesian coordinates (Cartesian) or in the lattice basis a_1, a_2, a_3 (Direct).

The second file is named KPOINTS, and it describes the k-space grid. The grid can be automatically generated by VASP or given explicitly by the user. An example of the first case is given below

```

1 Automatic mesh      # first line used as comment
2 0                  # 0 stands for automatically generated
3 Monkhorst Pack   # generation method
4 11 11 11           # number of k-points in each direction
5 0 0 0              # optional shift of the mesh

```

The zero in line 2 indicates that the grid has to be generated automatically with the generation method specified in line 3. Line 4 gives the number of points that have to be generated in every direction and line 5 an optional shift with respect to the centre of the Brillouin zone. In our example, a centered $11 \times 11 \times 11$ grid is generated.

For band structure calculation it is convenient to specify a custom grid. Instead of calculating the energy of the electrons for evenly-spaced k-points, some specific k-points of interest are chosen. Typically, they are special points of symmetry, like the centre of the Brillouin zone or the center of a side of the Fermi surface. An example is given below.

```

1 Bandstructure G-X-W-G          # first line used as comment
2 10                             # number of k-points per line
3 Line                            # line between the specified points
4 Reciprocal                      # Reciprocal or Cartesian
5 0.0 0.0 0.0 Gamma               # first point
6 0.5 0.5 0.0 X                 # second point
7
8 0.5 0.5 0.0 X                 # [...]
9 0.5 0.75 0.25 W
10
11 0.5 0.75 0.25 W
12 0.0 0.0 0.0 Gamma

```

In this example, three lines of 10 k-points are generated. The first goes from the point Γ to X, the second from X to W and the third from W to Γ . The number of points per line is defined in line 2. Like in the POSCAR, the points coordinates may be expressed in cartesian coordinates (Cartesian) or with respect to the reciprocal base b_1, b_2, b_3 (Reciprocal).

The last file that defines the system is named POTCAR. It contains all the information about the pseudopotentials that have to be used for the atoms in the cell. If more than one type of atom is present, multiple POTCARs are concatenated in a unique file. All the computational instructions, like the energy cut-off, are specified in the INCAR file. The INCAR file can contain a very vast number of parameters, of which giving a comprehensive description here would be impossible. We will present some of them in

the next chapter, when we need to use them. Finally, many output files are produced, among which there are: the OUTCAR, that contains all the details of the computation; the WAVECAR, that contains the final wavefunctions; the CHGCAR, that contains the final charge density. These last two files are particularly important if we want to start a simulation in the state in which another one ended.

SIMULATION OF A SMALL POLARON IN RUTILE

Rutile is the most common natural form of titanium dioxide (TiO_2). It is a material that has been vastly studied in the past decades [24]. It is known to be prone to the formation of small electron polarons, which give rise to an optically detected deep level below the conduction band. However, experiments seem to produce conflicting results: optical and spin-resonance techniques reveal strongly localized small polarons, while electrical measurements show high mobilities that can only be explained by delocalized free electrons. It was shown that small polarons can actually coexist with delocalized electrons in the conduction band of TiO_2 , the former being only slightly more energetically favoured over the latter [36].

In this chapter, we will discuss the simulation of a small polaron in rutile. The DFT+U simulation was run on a $3 \times 3 \times 3$ supercell on VASP. We will start by discussing the procedure that was followed to trap an extra electron in the TiO_2 supercell. Then, the resulting DOS and band structure will be discussed. Particular emphasis will be given to the comparison with a delocalized solution, with the electron in the conduction band.

4.1 PROCEDURE

In this section we present the procedure that was followed to trap a polaron in rutile. We start with a standard calculation on a rutile unit cell, followed by a DFT+U calculation. Then, we trap an extra electron in a supercell. We compute the properties of the polaron investigating the DOS and band structure. The calculation of a delocalized electron is discussed as well, and the two solutions are compared.

4.1.1 *DFT and DFT+U calculation on rutile*

We begin by performing a standard DFT calculation on rutile. To do so, we first need some information on the material we are investigating.

Rutile has a tetragonal unit cell, with two titanium and four oxygen atoms inside. A sketch of a unit cell is given in Fig. 3a. The lattice parameters and the positions of the atoms were taken from The Materials Project website [38] and inserted in the POSCAR file. The properties of the atoms, as we discussed in Section 3.2, are given by the pseudopotentials. For Ti, a projector augmented wave (PAW) pseudopotential with 12 electrons was used, whereas for O a PAW pseudopotential with 6 electrons was chosen. Finally, a k-points grid was generated. We chose to use a Γ -centered grid with

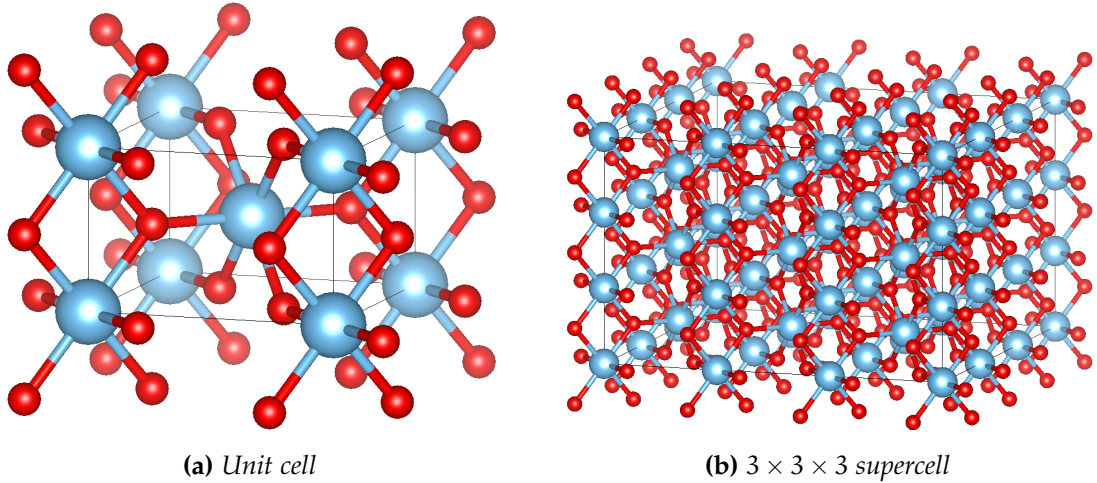


Figure 3: Rutile unit cell and supercell. Titanium is blue and oxygen is red. The images have been rendered with Vesta [37].

points separated by 0.03 \AA^{-1} . For the rutile unit cell, this was achieved by a $7 \times 7 \times 11$ grid. The necessary file was generated using Vaspkit [39].

With these settings, a series of DFT calculations was performed. In all the calculation we used a cut-off energy of 700 eV. The convergence was stopped when the energy difference of two successive electronic calculations was smaller than 1×10^{-8} eV and the forces on the ions smaller than 0.01 eV/Å. A Gaussian smearing with $\sigma = 0.05$ was used for the calculations that involved the relaxation of the system or the computation of the band structure. For the computation of the DOS, the tetrahedron method was chosen. In fact, the tetrahedron method usually gives better results, but it is not applicable to calculations where the position of the ions changes or with non-uniform k-points grids.

Before investigating the electronic properties of the material, we wanted to be sure that the structure we used was properly relaxed. A non-spin-polarized calculation was performed on the unit cell allowing the relaxation of the ions positions. The volume and the shape of the unit cell was kept constant, allowing the atomic positions to change. This is generally achieved by performing a series of standard electronic DFT calculations. Once the electronic charge converges, the forces on the ions is computed. The ions are then moved accordingly, minimizing the forces that act on them. Then, the next electronic calculation is run. The process stops once both the electronic and ionic calculations converge.

The relaxed structure was then used in a standard self-consistent DFT calculation. In particular, the DOS, the electronic charge density and the wavefunctions were computed. The result was used in a non-selfconsistent calculation to compute the band structure. The bands were calculated along a special path of k-points. Conventionally, these points are named Γ -X-M- Γ -Z-R-A-Z; X-R; M-A. They are high-symmetry points of the first

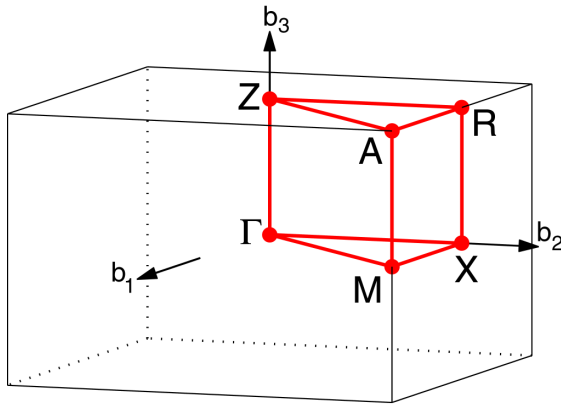


Figure 4: Brillouin zone of a tetragonal system, the red path passes through the high-symmetry points of the zone. $\mathbf{b}_1, \mathbf{b}_2, \mathbf{b}_3$ are the reciprocal basis vectors of a tetragonal unit cell. The path used in the calculation of the band structure was $\Gamma\text{-}X\text{-}M\text{-}\Gamma\text{-}Z\text{-}R\text{-}A\text{-}Z$; $X\text{-}R$; $M\text{-}A$.

Brillouin zone of a tetragonal system. The position of the points in the Brillouin zone is displayed in Fig. 4. Each high-symmetry k-point was connected with a line of 10 k-points to the next one.

As discussed in Section 3.1.3, DFT often fails to give appropriate results in band-gap calculations. To correct the problem, the previous calculations were repeated in the DFT+U approach. The DFT+U correction was implemented following the Duradev approach, setting the value of U to 3.9 eV [40]. The correction was applied to the d-orbitals of titanium, leaving the other orbitals unaltered. Starting from the relaxed structure, we relaxed it again with the DFT+U correction. The DOS and band structure were computed as well, following the same procedure described above.

4.1.2 Electron localization

To find a polaronic solution, we had to add an extra electron to the system and localize it at the centre of the cell. Since the electron must be localized in a region of the size of a unit cell, the simulation cannot be run on a unit cell alone. The unit cell is repeated in the crystal, so the polaron would interfere with itself at the cell boundaries, resulting in self-interaction errors. To solve this problem, the unit cell is replaced with a supercell, which is a cell made by the repetition of a unit cell. For this reason, only small polarons can be simulated in DFT. For large polarons, the supercell size would be too big to be simulated.

A $3 \times 3 \times 3$ supercell was created with the Vesta software [37], repeating the relaxed unit cell three times in each direction. A sketch of the supercell is reported in Fig. 3b. The unit cell that was repeated was the result of the relaxation performed with the DTF+U correction. The usual calculations described above were performed on the

supercell, computing the DOS and the band structure. Moreover, the number of electrons present in the system was noted. Knowing the number of electrons is useful to trap an extra electron in the supercell.

Since the formation of the polaron is only slightly energetically favoured compared to a delocalized solution, the extra electron is difficult to localize. Simply adding one electron to the system does not result in a localized state.

To find a localized solution, a more gradual approach was necessary. The central titanium atom was substituted with vanadium. Vanadium is the element following titanium in the periodic table, so it has one more electron and a stronger nuclear attraction. The substitution was done modifying the POSCAR and POTCAR files. For vanadium, a PAW pseudopotential with 13 electrons was used.

Added the electron, a number of expedients was needed to ensure that the electron was localized. The aim was to localize it on the central atom, the vanadium one. The six oxygen atoms around the central atom were moved outwards by 0.04 \AA , creating a potential well for the electron. Moreover, the $U - J$ value was set to 3.9 eV for titanium d-orbitals and to 9 eV for vanadium d-orbitals. Together, the stronger nuclear attraction of the vanadium atom, the displacement of the oxygen atoms, and the high $U - J$ value, favoured the electron localization at the centre of the supercell.

A DFT+U calculation was run allowing lattice relaxations. The extra electron in the system introduced a spin magnetic moment, so the calculation was spin-polarized. The magnetic moment was initially set to zero for every atom except for the vanadium one, which was set to $+\mu_B$, where μ_B is the Bohr magneton. To check if the electron was localized, the magnetic moment of the atoms was read in the output. For a localized state, we expected the central vanadium atom to be the only one with a magnetic moment of the order of μ_B .

The localized solution was used to initialize a new set of calculations. The goal was to gradually substitute the vanadium atom with a high $U - J$ value with a titanium atom with a normal $U - J$ value. This was done in two steps.

Firstly, vanadium was removed and titanium was placed back, leaving the $U - J$ value applied to the central atom unchanged. To keep the electron in the system, the number of electrons was manually set to the same number of the calculation with vanadium. The atomic positions were set as in the previous calculations, with the oxygen atoms shifted by 0.04 \AA . The calculation was initialized with the charge density and wavefunctions obtained from the system with vanadium, where the electron was already localized. The calculation was spin-polarized, and the initial magnetic moment was read from the charge density file. The localization of the electron was checked looking at the magnetic moment as explained above. Moreover, the eigenvalues and DOS were also inspected to see if a new state was present in the middle of the band gap.

Secondly, the calculation of the polaron was done continuing the last calculation with a normal $U - J$ value for the central titanium atom. The calculation was initialized with

the atomic positions, charge density and wavefunctions of the previous calculation. The magnetic moments, DOS and eigenvalues were inspected again to check if the polaron was still present.

4.1.3 Polaron

Some last calculations were run to compute the polaron properties. An electronic calculation without relaxation was done starting from the previous result to compute a more precise DOS. The band structure of the polaronic solution was also computed with a non-self-consistent calculation on the usual path of k-points. Finally, the isosurfaces of the charge density of the polaron was computed. To do so, the charge was decomposed over the different bands, and the polaronic band was selected restricting the calculation to an appropriate energy interval. The final result was rendered with Vesta, and the electron localization observed.

A delocalized solution was computed as well for comparison. To achieve this, an extra electron was added to the supercell and a non-spin-polarized DFT+U calculation was performed. The extra electron was added manually, setting the number of electrons to the number of the electrons in the original rutile supercell plus one. The DOS and band structure were computed as usual.

4.2 RESULTS

4.2.1 DFT and DFT+U calculation on rutile

In this section, we present the results of the calculations described above. We start by discussing the results of the calculations on the unit cell, confronting the standard DFT and DFT+U approaches. We then look at the results of the supercell with an extra electron, comparing the delocalized solution with the formation of the polaron.

The results of the calculations on the unit cell are reported in Fig. 5. The band gap between the valence and conduction band is immediately visible, both in the band structure diagram and in the DOS plot. The energy scale is shifted to have the zero at the top of the valence band. At 0 K, all the electrons are in the valence band, under the band gap.

The band gap is found to be direct, meaning that both the top of the valence band and the bottom of the conduction band are found in correspondence of the Γ k-point. As expected, the gap is larger in the DFT+U calculation. The standard DFT calculation returned a band gap of 1.83 eV, whereas the DFT+U calculation a band gap of 2.33 eV.

We expected the results of the calculation on the supercell, without the extra electron, to be similar to the results of the unit cell. The band structure and the DOS of the rutile supercell is displayed in Fig. 6. It is immediately visible that in the supercell many more bands are accessible. This is due to the bigger number of atoms. Each atom contribute

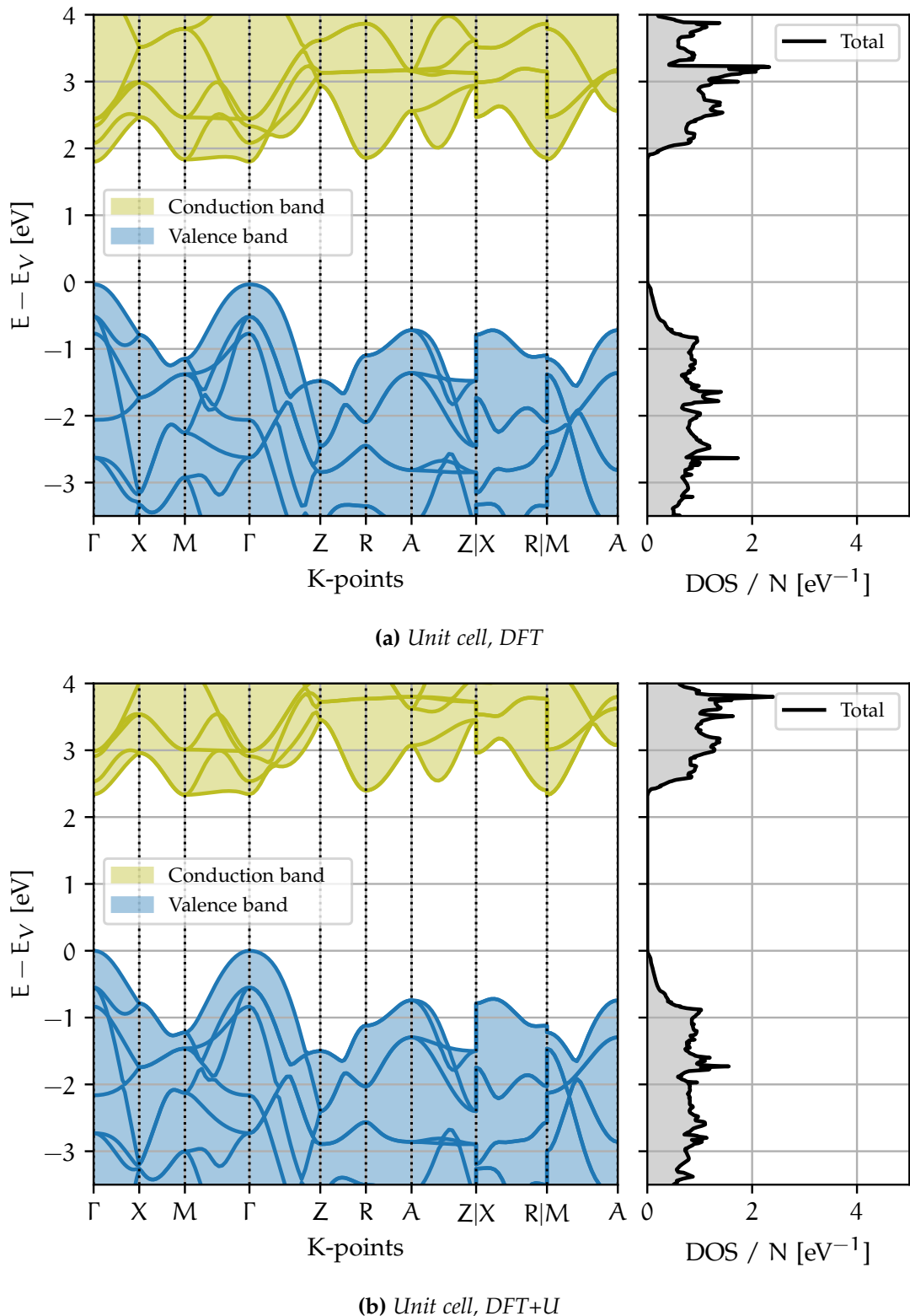


Figure 5: Band structure and DOS of the TiO_2 rutile unit cell. The zero of the energy scale is set to the energy of the top of valence band E_V . The DOS is divided by the total number of atoms $N = 6$. The direct ($\Gamma - \Gamma$) band gap in (a) is 1.83 eV, whereas in (b) it is 2.33 eV.

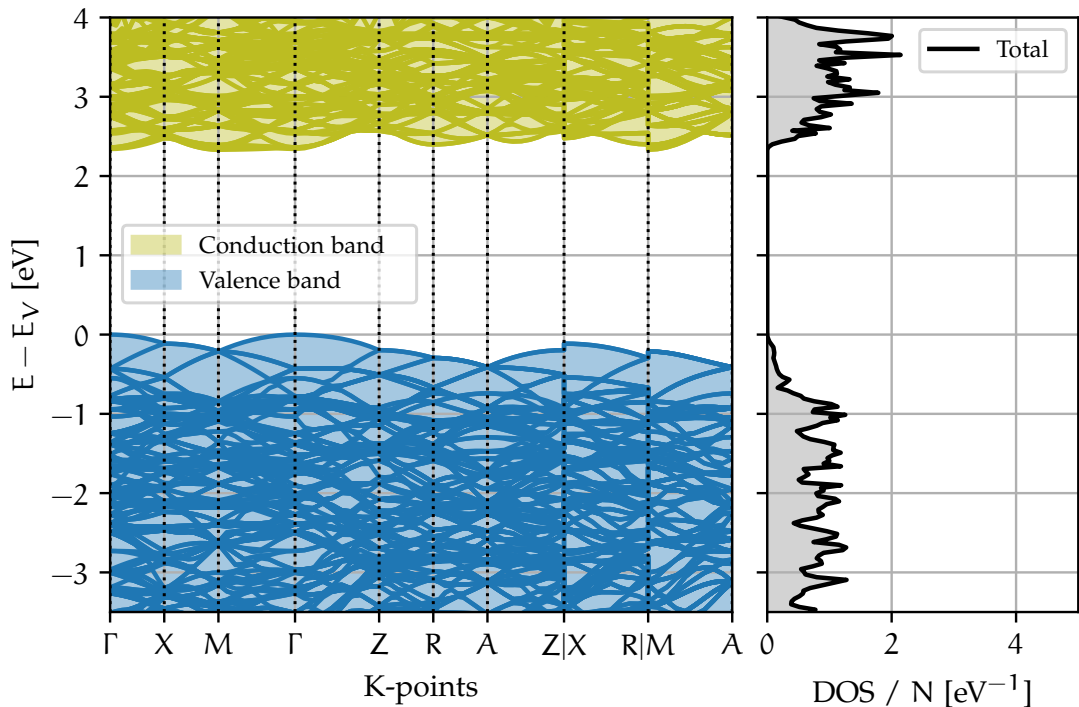


Figure 6: Band structure and DOS of the TiO_2 rutile supercell. The zero of the energy scale is set to the energy of the top of valence band E_V . The DOS is divided by the total number of atoms $N = 162$.

to the band structure with its own atomic orbitals and electrons, so it is natural to have more bands with more atoms. Band-unfolding techniques have been developed to overcome this inconvenience, reducing the supercell band structure diagram to the unit cell one [41]. However, since the exact band structure of rutile was not the main focus of this work, this was not done. Nevertheless, in Fig. 6 we can still clearly see a band gap and a DOS similar to the ones observed in Fig. 5b. In both diagrams, the DOS has been divided by the total number of atoms to make the results comparable.

4.2.2 Electron localization

We now briefly look at the results of the process of localizing the extra electron at the centre of the cell.

Substituting the titanium atom in the middle of the cell with a vanadium atom with a high U-value resulted in a well localized electron at the center of the cell. Observing the resulting eigenvalues, a new state with spin $+μ_B$ was found in the conduction band. The magnetic moments of the atoms were all zero except for the vanadium one. The central vanadium atom had a magnetic moment of $1.093\mu_B$.

Once we succeeded in localizing the electron, we had to replace the vanadium atom with the original titanium one. With the titanium atom, and a high U-value, the extra electron remained localized. This was confirmed by a magnetic moment on the central atom of $0.930\mu_B$ and an extra state in the valence band. Finally, setting $U - J$ to 3.9 eV for the central titanium atom, the final polaron state was found. The magnetic moment on the central atom was $0.787\mu_B$ and a new state was created 0.70 eV under the conduction band (in correspondence of the Γ k-point).

4.2.3 Polaron

The DOS and the band structure of the polaronic solution are displayed in Fig. 7a. An extra state is clearly visible both in the DOS and in the band structure, 0.70 eV below the conduction band in correspondence of the Γ point. In the DOS diagram, the total DOS has been plotted together with the projection of the DOS on the central titanium atom. It is interesting to pay attention to the region between -0.2 eV and 0.0 eV, which is the energy region of the polaron. Here, most of the contribution to the total DOS is given by the projection on the central atom. This means that the electron is mostly localized on this atom. In other energy regions, the central atom contributes to the total DOS as every other atom, so on average for $1/N$ where $N = 162$ is the total number of atoms in the supercell.

The aforementioned plot has to be compared with the diagram in Fig. 7b. Here, it is displayed the delocalized solution. We notice that this time the electron enters the conduction band, and no new state is created in the middle of the energy gap. This is confirmed by the DOS. We see that some states just below 0.0 eV are filled by the extra electron. The central atom contribution to the total DOS is not as relevant as before. This is compatible with an electron delocalized in the material, with all the atoms contributing in equal amounts to the total DOS.

The two cases can also be compared looking at the charge isosurfaces. To focus on the extra electron charge density, we have projected the total charge density on the band of the extra electron. The result is displayed in Figs. 8 and 9. In the first figure, the entire supercell is shown, whereas in the second one only the central atom with the six nearest-neighbours oxygen atoms. From Fig. 8a it is clearly visible how in the polaronic case the charge is localized in the centre of the supercell. The exact shape of the charge isosurface is better visible in Fig. 9a. Here it is also emphasized how the localization of the charge is possible only thanks to the displacement of the oxygen atoms. The four oxygen atoms closer to the titanium atom are displaced by 0.085\AA outwards, whereas the two further oxygen atoms by 0.023\AA . In the delocalized case, displayed in Figs. 8b and 9b, the electron is delocalized on both the titanium and oxygen atoms.

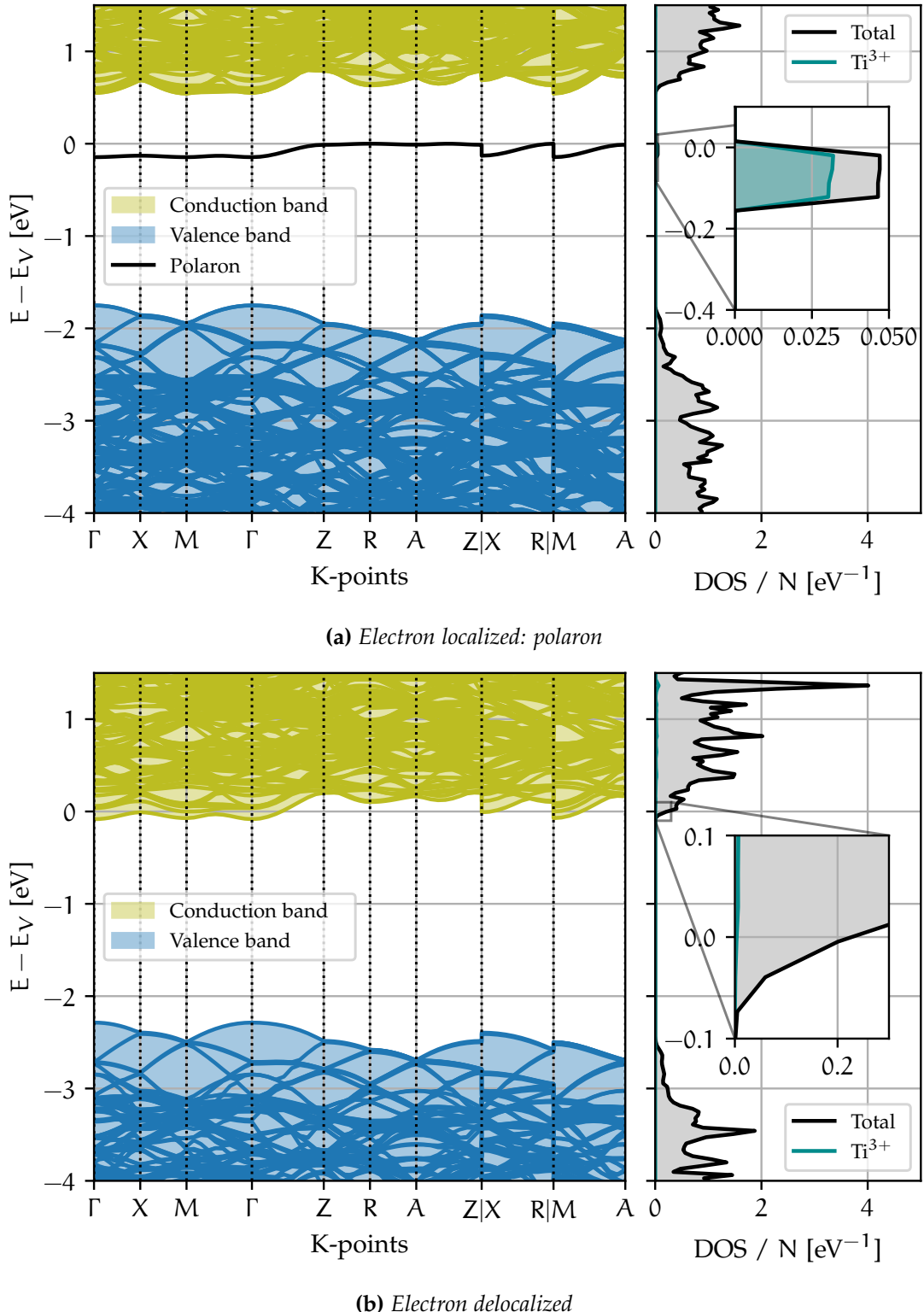


Figure 7: Band structure and DOS of the TiO_2 rutile supercell with an extra electron. The zero of the energy scale is set to the energy of the top of valence band E_V . The DOS is divided by the total number of atoms $N = 162$. In (a) in addition to the total DOS, the partial DOS of the central atom - where the electron is localized - is reported as well.

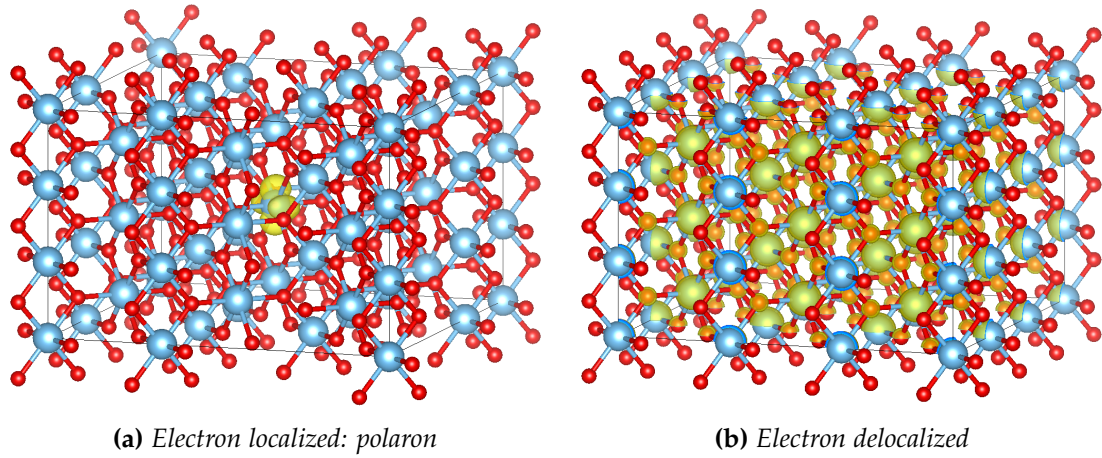


Figure 8: Supercell with the isosurface of the charge density projected on the extra-electron band. In (a) the extra electron is localized and forms a polaron, in (b) it is delocalized. The blue atoms are titanium atoms, whereas the red ones oxygen atoms.

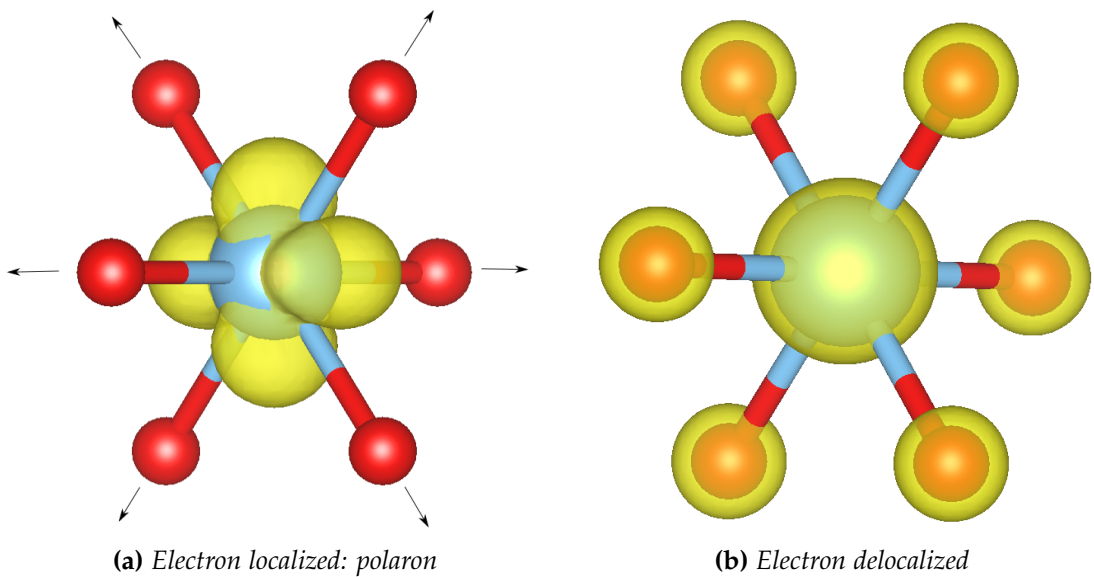


Figure 9: Central atom with the isosurface of the charge density projected on the extra-electron band. In (a) the extra electron is localized and forms a polaron, in (b) it is delocalized. The blue atom is the central titanium atom, whereas the red ones are the nearest-neighbours oxygen atoms.

5

CONCLUSIONS

BIBLIOGRAPHY

- [1] "Electron Motiton in Crystal Lattice". In: *Collected Papers of L.D. Landau*. Ed. by D. Ter haar. Pergamon, Jan. 1, 1965, pp. 67–68. ISBN: 978-0-08-010586-4. DOI: [10.1016/B978-0-08-010586-4.50015-8](https://doi.org/10.1016/B978-0-08-010586-4.50015-8).
- [2] Solomon Pekar. "Local Quantum States of Electrons in an Ideal Ion Crystal". In: *Zhurnal Eksperimentalnoi i Teoreticheskoi Fiziki* 16.4 (1946), pp. 341–348.
- [3] S. I. Pekar. "Theory of Colored Crystals". In: *Zhurnal Eksperimentalnoi i Teoreticheskoi Fiziki* 17 (1947), p. 868.
- [4] L. D. Landau and S. I. Pekar. "Effective Mass of a Polaron". In: *Zh. Eksp. Teor. Fiz.* 18.5 (1948), pp. 419–423.
- [5] Herbert Fröhlich, Hans Pelzer, and Sigurd Zienau. "XX. Properties of Slow Electrons in Polar Materials". In: *The London, Edinburgh, and Dublin Philosophical Magazine and Journal of Science* 41.314 (1950), pp. 221–242.
- [6] Th Holstein. "Studies of Polaron Motion: Part I. The Molecular-Crystal Model". In: *Annals of physics* 8.3 (1959), pp. 325–342.
- [7] Han Rongsheng, Lin Zijing, and Wang Kelin. "Exact Solutions for the Two-Site Holstein Model". In: *Physical Review B* 65.17 (Apr. 16, 2002), p. 174303. DOI: [10.1103/PhysRevB.65.174303](https://doi.org/10.1103/PhysRevB.65.174303).
- [8] Nikolai V. Prokof'ev and Boris V. Svistunov. "Polaron Problem by Diagrammatic Quantum Monte Carlo". In: *Physical Review Letters* 81.12 (Sept. 21, 1998), pp. 2514–2517. DOI: [10.1103/PhysRevLett.81.2514](https://doi.org/10.1103/PhysRevLett.81.2514).
- [9] A. S. Mishchenko et al. "Diagrammatic Quantum Monte Carlo Study of the Fröhlich Polaron". In: *Physical Review B* 62.10 (Sept. 1, 2000), pp. 6317–6336. DOI: [10.1103/PhysRevB.62.6317](https://doi.org/10.1103/PhysRevB.62.6317).
- [10] Sebastian Kokott et al. "First-Principles Supercell Calculations of Small Polarons with Proper Account for Long-Range Polarization Effects". In: *New Journal of Physics* 20.3 (Mar. 2018), p. 033023. ISSN: 1367-2630. DOI: [10.1088/1367-2630/aaaaf44](https://doi.org/10.1088/1367-2630/aaaaf44).
- [11] Weng Hong Sio et al. "Polarons from First Principles, without Supercells". In: *Physical Review Letters* 122.24 (June 19, 2019), p. 246403. DOI: [10.1103/PhysRevLett.122.246403](https://doi.org/10.1103/PhysRevLett.122.246403).
- [12] P. A. M. Dirac. "The Quantum Theory of the Emission and Absorption of Radiation". In: *Proceedings of the Royal Society of London Series A* 114 (Mar. 1, 1927), pp. 243–265. ISSN: 0080-46301364-5021. DOI: [10.1098/rspa.1927.0039](https://doi.org/10.1098/rspa.1927.0039).

- [13] V. Fock. "Konfigurationsraum und zweite Quantelung". In: *Zeitschrift für Physik* 75.9 (Sept. 1, 1932), pp. 622–647. ISSN: 0044-3328. DOI: [10.1007/BF01344458](#).
- [14] J. J. Sakurai and Jim Napolitano. *Modern Quantum Mechanics*. Cambridge University Press, Sept. 17, 2020. 571 pp. ISBN: 978-1-108-47322-4.
- [15] A. Sommerfeld. "Zur Elektronentheorie der Metalle auf Grund der Fermischen Statistik". In: *Zeitschrift für Physik* 47.1 (Jan. 1, 1928), pp. 1–32. ISSN: 0044-3328. DOI: [10.1007/BF01391052](#).
- [16] P. Drude. "Zur Elektronentheorie Der Metalle; II. Teil. Galvanomagnetische Und Thermomagnetische Effecte". In: *Annalen der Physik* 308.11 (1900), pp. 369–402. ISSN: 1521-3889. DOI: [10.1002/andp.19003081102](#).
- [17] Felix Bloch. "Über die Quantenmechanik der Elektronen in Kristallgittern". In: *Zeitschrift für Physik* 52.7 (July 1, 1929), pp. 555–600. ISSN: 0044-3328. DOI: [10.1007/BF01339455](#).
- [18] Marvin L. Cohen and Steven G. Louie. *Fundamentals of Condensed Matter Physics*. 1st ed. Cambridge University Press. ISBN: 978-0-521-51331-9.
- [19] Jacques Tempere. *Advanced Electronic Structures*. Universiteit Antwerpen.
- [20] Charles Kittel. *Quantum Theory of Solids*. Wiley, Apr. 2, 1987. 528 pp. ISBN: 978-0-471-62412-7.
- [21] A. S Alexandrov and J. T Devreese. *Advances in Polaron Physics*. Heidelberg; New York: Springer, 2010. ISBN: 978-3-642-01896-1.
- [22] Amin Tayebi and Vladimir Zelevinsky. "The Holstein Polaron Problem Revisited". In: *Journal of Physics A: Mathematical and Theoretical* 49.25 (May 2016), p. 255004. ISSN: 1751-8121. DOI: [10.1088/1751-8113/49/25/255004](#).
- [23] Yuriy Natanzon, Amram Azulay, and Yaron Amouyal. "Evaluation of Polaron Transport in Solids from First-principles". In: *Israel Journal of Chemistry* 60.8-9 (2020), pp. 768–786. ISSN: 1869-5868. DOI: [10.1002/ijch.201900101](#).
- [24] Cesare Franchini et al. "Polarons in Materials". In: *Nature Reviews Materials* 6.7 (July 1, 2021), pp. 560–586. ISSN: 2058-8437. DOI: [10.1038/s41578-021-00289-w](#).
- [25] P. Hohenberg and W. Kohn. "Inhomogeneous Electron Gas". In: *Physical Review* 136 (3B Nov. 9, 1964), B864-B871. DOI: [10.1103/PhysRev.136.B864](#).
- [26] W. Kohn and L. J. Sham. "Self-Consistent Equations Including Exchange and Correlation Effects". In: *Physical Review* 140 (4A Nov. 15, 1965), A1133–A1138. DOI: [10.1103/PhysRev.140.A1133](#).
- [27] A. Seidl et al. "Generalized Kohn-Sham Schemes and the Band-Gap Problem". In: *Physical Review B* 53.7 (Feb. 15, 1996), pp. 3764–3774. DOI: [10.1103/PhysRevB.53.3764](#).

- [28] Sarah Tolba et al. "The DFT+U: Approaches, Accuracy, and Applications". In: May 16, 2018. ISBN: 978-1-78923-132-8. DOI: [10.5772/intechopen.72020](https://doi.org/10.5772/intechopen.72020).
- [29] Vladimir I. Anisimov, Jan Zaanen, and Ole K. Andersen. "Band Theory and Mott Insulators: Hubbard U Instead of Stoner I". In: *Physical Review B* 44.3 (July 15, 1991), pp. 943–954. DOI: [10.1103/PhysRevB.44.943](https://doi.org/10.1103/PhysRevB.44.943).
- [30] S. L. Dudarev et al. "Electron-Energy-Loss Spectra and the Structural Stability of Nickel Oxide: An LSDA+U Study". In: *Physical Review B* 57.3 (Jan. 15, 1998), pp. 1505–1509. DOI: [10.1103/PhysRevB.57.1505](https://doi.org/10.1103/PhysRevB.57.1505).
- [31] Hendrik J. Monkhorst and James D. Pack. "Special Points for Brillouin-zone Integrations". In: *Physical Review B* 13.12 (June 15, 1976), pp. 5188–5192. DOI: [10.1103/PhysRevB.13.5188](https://doi.org/10.1103/PhysRevB.13.5188).
- [32] G. Kresse and J. Hafner. "Ab Initio Molecular Dynamics for Liquid Metals". In: *Physical Review B* 47.1 (Jan. 1, 1993), pp. 558–561. DOI: [10.1103/PhysRevB.47.558](https://doi.org/10.1103/PhysRevB.47.558).
- [33] G. Kresse and J. Furthmüller. "Efficiency of Ab-Initio Total Energy Calculations for Metals and Semiconductors Using a Plane-Wave Basis Set". In: *Computational Materials Science* 6.1 (July 1, 1996), pp. 15–50. ISSN: 0927-0256. DOI: [10.1016/0927-0256\(96\)00008-0](https://doi.org/10.1016/0927-0256(96)00008-0).
- [34] G. Kresse and J. Furthmüller. "Efficient Iterative Schemes for Ab Initio Total-Energy Calculations Using a Plane-Wave Basis Set". In: *Physical Review B* 54.16 (Oct. 15, 1996), pp. 11169–11186. DOI: [10.1103/PhysRevB.54.11169](https://doi.org/10.1103/PhysRevB.54.11169).
- [35] G. Kresse and D. Joubert. "From Ultrasoft Pseudopotentials to the Projector Augmented-Wave Method". In: *Physical Review B* 59.3 (Jan. 15, 1999), pp. 1758–1775. DOI: [10.1103/PhysRevB.59.1758](https://doi.org/10.1103/PhysRevB.59.1758).
- [36] A. Janotti et al. "Dual Behavior of Excess Electrons in Rutile TiO₂". In: *physica status solidi (RRL) – Rapid Research Letters* 7.3 (2013), pp. 199–203. ISSN: 1862-6270. DOI: [10.1002/pssr.201206464](https://doi.org/10.1002/pssr.201206464).
- [37] VESTA. URL: <https://jp-minerals.org/vesta/en/> (visited on 04/26/2022).
- [38] Kristin Persson. *Materials Data on TiO₂ (SG:136) by Materials Project*. United States, Nov. 2014. DOI: [10.17188/1184648](https://doi.org/10.17188/1184648).
- [39] Wei Wang et al. "VASPKIT: A User-Friendly Interface Facilitating High-Throughput Computing and Analysis Using VASP Code". In: *Computer Physics Communications* 267 (2021), p. 108033. DOI: [10.1016/j.cpc.2021.108033](https://doi.org/10.1016/j.cpc.2021.108033).
- [40] Michele Reticcioli, Ulrike Diebold, and Cesare Franchini. "Modeling Polarons in Density Functional Theory: Lessons Learned from TiO₂". In: *Journal of Physics: Condensed Matter* 34.20 (May 18, 2022), p. 204006. ISSN: 0953-8984, 1361-648X. DOI: [10.1088/1361-648X/ac58d7](https://doi.org/10.1088/1361-648X/ac58d7).

- [41] Sara G. Mayo, Felix Yndurain, and Jose M. Soler. "Band Unfolding Made Simple". In: *Journal of Physics: Condensed Matter* 32.20 (Feb. 2020), p. 205902. ISSN: 0953-8984.
DOI: [10.1088/1361-648X/ab6e8e](https://doi.org/10.1088/1361-648X/ab6e8e).